

RESEARCH ARTICLE

Noise improves the association between effects of local stimulation and structural degree of brain networks

Yi Zheng^{1,3}, Shaoting Tang^{2,3,4,5,6,7,8,9*}, Hongwei Zheng^{10*}, Xin Wang^{2,3,4,5,6,7}, Longzhao Liu^{2,3,4,5,6,7}, Yaqian Yang^{1,3}, Yi Zhen^{1,3}, Zhiming Zheng^{2,3,4,5,6,7,8,9}

1 School of Mathematical Sciences, Beihang University, Beijing, China, **2** Institute of Artificial Intelligence, Beihang University, Beijing, China, **3** Key laboratory of Mathematics, Informatics and Behavioral Semantics (LMIB), Beihang University, Beijing, China, **4** State Key Lab of Software Development Environment (NLSDE), Beihang University, Beijing, China, **5** Zhongguancun Laboratory, Beijing, P.R. China, **6** Beijing Advanced Innovation Center for Future Blockchain and Privacy Computing, Beihang University, Beijing, China, **7** PengCheng Laboratory, Shenzhen, China, **8** Institute of Medical Artificial Intelligence, Binzhou Medical University, Yantai, China, **9** School of Mathematical Sciences, Dalian University of Technology, Dalian, China, **10** Beijing Academy of Blockchain and Edge Computing (BABEC), Beijing, China

* tangshaoting@buaa.edu.cn (ST); hwzheng@pku.edu.cn (HZ)



OPEN ACCESS

Citation: Zheng Y, Tang S, Zheng H, Wang X, Liu L, Yang Y, et al. (2023) Noise improves the association between effects of local stimulation and structural degree of brain networks. *PLoS Comput Biol* 19(5): e1010866. <https://doi.org/10.1371/journal.pcbi.1010866>

Editor: Hayriye Cagnan, University of Oxford, UNITED KINGDOM

Received: January 10, 2023

Accepted: April 20, 2023

Published: May 11, 2023

Copyright: © 2023 Zheng et al. This is an open access article distributed under the terms of the [Creative Commons Attribution License](https://creativecommons.org/licenses/by/4.0/), which permits unrestricted use, distribution, and reproduction in any medium, provided the original author and source are credited.

Data Availability Statement: The structural data is available at https://github.com/lia-papadopoulos/WilsonCowan_DynamicalState_Stim. The Matlab code for main simulations is available at <https://github.com/Yibh22/noise-influences-stimulation-effects>.

Funding: ST is funded by the National Key R&D Program of China Grant No. 2022ZD0116800, Program of National Natural Science Foundation of China Grant No. 11871004 and Program of National Natural Science Foundation of China Grant

Abstract

Stimulation to local areas remarkably affects brain activity patterns, which can be exploited to investigate neural bases of cognitive function and modify pathological brain statuses. There has been growing interest in exploring the fundamental action mechanisms of local stimulation. Nevertheless, how noise amplitude, an essential element in neural dynamics, influences stimulation-induced brain states remains unknown. Here, we systematically examine the effects of local stimulation by using a large-scale biophysical model under different combinations of noise amplitudes and stimulation sites. We demonstrate that noise amplitude nonlinearly and heterogeneously tunes the stimulation effects from both regional and network perspectives. Furthermore, by incorporating the role of the anatomical network, we show that the peak frequencies of unstimulated areas at different stimulation sites averaged across noise amplitudes are highly positively related to structural connectivity. Crucially, the association between the overall changes in functional connectivity as well as the alterations in the constraints imposed by structural connectivity with the structural degree of stimulation sites is nonmonotonically influenced by the noise amplitude, with the association increasing in specific noise amplitude ranges. Moreover, the impacts of local stimulation of cognitive systems depend on the complex interplay between the noise amplitude and average structural degree. Overall, this work provides theoretical insights into how noise amplitude and network structure jointly modulate brain dynamics during stimulation and introduces possibilities for better predicting and controlling stimulation outcomes.

No. 11922102; XW is funded by the Program of National Natural Science Foundation of China Grant No. 12201026; ZZ is funded by the Program of National Natural Science Foundation of China Grant No. 62141605. The funders had no role in study design, data collection and analysis, decision to publish, or preparation of the manuscript.

Competing interests: The authors have declared that no competing interests exist.

Author summary

Despite the extensive application of local stimulation in cognition research and disease treatments, how regional perturbations alter brain-wide dynamics has not yet been fully understood. Given that noninvasive stimulation is associated with changes in the signal-noise relationship, we assume that noise amplitude is one of the plausible factors modulating the stimulation effects. Using a whole-brain biophysical model under different stimulation sites and noise amplitudes, we explore the influence of noise amplitude on stimulation effects and, more importantly, the interplay between noise amplitude and network structure. From a regional perspective, noise amplitude reduces the peak frequencies in unstimulated areas during stimulation. Moreover, we find a high similarity between the noise-averaged peak frequency matrix and the structural network. From a network perspective, we show that the changes in functional connectivity are decreased by noise amplitude, while the alterations in structural constraints display nonmonotonic trends. Intriguingly, increasing the noise amplitude in specific ranges can improve the association between network-level effects and structural degree, promoting better predicting and controlling therapeutic performance. Finally, the behaviors of cognitive systems quantified by network-level effects are jointly modulated by the noise amplitude and average structural degree.

Introduction

Complex interactions among brain areas elicit the rich spatiotemporal profiles of neural activity that underlie human cognition and behaviors [1, 2]. Because the brain is an open system, typical brain activity patterns are highly influenced by local perturbations, yielding various dynamical states [3]. For example, sensory inputs can be viewed as local stimulation that induces neural activity changes in primary areas. These changes subsequently affect the associative cortex through neural circuits, enabling sophisticated cognitive processes such as learning, decision-making and memory [4–6]. In addition, aberrant statuses caused by certain brain disorders are associated with local perturbations. Specifically, some generalized epileptic seizures are caused by stimulus-induced abnormal activity in focal areas spreading throughout the brain [7, 8]. Despite the critical role of local perturbations, how regional stimulation modulates the underlying neural processes has not yet been fully established [9].

Since their inception, artificial stimulation techniques have served as efficient tools that allow researchers to directly investigate responses to experimentally altered local neural activity. These methods have been widely used to explore the causal relationship between select brain regions and cognitive processes or task behaviors [10]. Moreover, they are promising for the treatment of psychiatric and neurological disorders. Deep brain stimulation (DBS) and transcranial magnetic stimulation (TMS) are two commonly used techniques. DBS involves implanting electrodes in specific brain regions and is frequently used for patients with Parkinson's disease, Alzheimer's disease and dementia [11–13]. The non-invasive TMS utilizes magnetic fields to stimulate specific brain areas and is often employed for treating epilepsy, autism and schizophrenia [14–16]. Revealing the effects of local stimulation may improve our understanding of the neurodynamic bases of human cognition and behaviors and facilitate the development and utilization of stimulation techniques.

It has been widely accepted that local perturbations not only induce regional modifications near stimulation sites but also provoke broad system-level impacts [10, 17, 18]. Researchers have focused on how anatomical connectivity constrains global stimulation effects, given that

neural activity propagates along white matter bundles. They have found the vital contribution of macroscale structural properties such as degrees and modules [19, 20]. Moreover, recent studies have demonstrated that stimulation effects rely on physiological and cognitive states [21, 22]. Sleep or working memory states generate specific neural activity patterns that differ from the resting state. These patterns alter the transmission of local stimulation, leading to changes in the regional power spectra, interregional functional coupling and behavioral performance [23, 24]. Despite these advances, our understanding of brain stimulation remains incomplete, such as the high variability of stimulation outcomes across subjects [25, 26]. This suggests that further research is required to understand the fundamental mechanisms underlying how regional activity changes influence brain-wide dynamics. Activity patterns elicited by stimulation should be jointly modulated by multiple neurophysiological factors. For example, recent research showed that the response to local perturbations depends on both the stimulation sites and oscillatory states of brain network activity [27]. Nevertheless, most studies have tended to examine the impact of single elements, thus overlooking other factors that may have vital influences on network communication and ignoring the essential interplay among these factors.

Neural noise, including multiple sources such as sensory, cellular and electrical noise, affects all aspects of the behaviors of the nervous system [28]. On the one hand, neural noise is thought to hinder information processing and transmission. On the other hand, neural noise has been found to help maintain and promote brain function, including shaping resting-state functional networks [29, 30], enhancing neural synchronization [31, 32] and affecting task performance [33, 34]. In addition, previous research has indicated that the brain, as a noisy dynamical system, manifests subject-specific parameters at various scales, thus producing diverse outputs [28, 35]. Moreover, a recent study has linked local stimulation to noise amplitude, demonstrating that noninvasive brain stimulation could be viewed as a neural activity modification that alters the signal-noise relationship [36]. Based on this evidence, we assume that neural noise is a crucial factor that influences stimulation-induced brain states. However, how the noise amplitude is related to the global consequences of local stimulation remains unknown. In particular, despite the previously revealed contribution of network structure, the interplay between noise amplitude and network structure remains unexplored.

Experimentally examining the effects of local stimulation across different parameters is impractical, time-consuming and potentially detrimental to participants; however, model-based numerical simulation offers a powerful approach to investigating these unknown situations [27, 37–41]. Thus, in the present work, we utilize a whole-brain biophysical model composed of Wilson-Cowan neural masses to systematically explore dynamic brain states at different stimulation sites under various noise amplitudes. We first select an appropriate global coupling strength independent of the noise amplitude before stimulation. Then, we evaluate the stimulation effects by examining the frequencies associated with the maximum values in the regional power spectrum (peak frequencies), the changes in the functional configurations (functional effects) and the alterations in the structural constraints on function (structural effects) [37].

From the regional perspective, we show that the noise amplitude influences the peak frequencies of unstimulated brain areas, shifting the frequencies from higher to lower values. Moreover, we find a high positive association between the peak frequencies of unstimulated areas at different stimulation sites averaged across noise amplitudes and the corresponding structural connectivity, underlining the antagonistic effects of the direct connection strength and noise amplitude. From the network perspective, we show that functional effects are nonlinearly weakened by noise amplitude, while structural effects exhibit trends of first increasing and then decreasing under specific amplitude ranges. As a result of the heterogeneous impact

of noise amplitude on stimulation sites, increasing the noise amplitude in specific ranges can enhance both the Pearson correlation coefficient and the adjusted coefficient of determination between the functional or structural effects and the structural degree of stimulation sites. The changes in the noise amplitude can even turn the correlation of structural effects from negative to positive. Finally, we show that the noise amplitude and system-level average degree jointly modulate the performance of cognitive systems in terms of functional and structural effects. The subcortical system with a high average degree exhibits distinct behaviors under various noise amplitudes from the sensory and association system with a low average degree. In summary, our study highlights the significance of the coupling between noise amplitude and network structure in modulating the effects of regional stimulation. It provides valuable insights into the fundamental principles of brain dynamics, potentially facilitating the development of personalized stimulation techniques and the optimization of therapeutic outcomes.

Methods

General workflow

We utilize a three-step investigation procedure that consists of input data, computational model and analysis scheme (Fig 1). Briefly, the input data of the procedure include the group-level structural connectivity matrix, group-level distance matrix and stimulation protocol (Fig 1A–1C). The computational model is illustrated by a single trial involving local perturbation to the brain network (Fig 1D), the Wilson-Cowan dynamics between brain regions (Fig 1E) and the main simulations under different combinations of noise amplitudes and stimulation sites (Fig 1F). Finally, the firing rates of all excitatory populations during 1–2 s and 2–3 s are extracted as time series before and during stimulation (Fig 1G). The regional power spectra and functional connectivity matrices are estimated to evaluate the effects of local stimulation (Fig 1H and 1I).

Input data

We utilize a group-level anatomical brain network mentioned in a previous study [27], which is derived by implementing deterministic tractography algorithms for diffusion-weighted MRI of 30 healthy subjects (mean age 26.2 years, the standard deviation 5.7 years, 14 female subjects) [42, 43]. The weighted and undirected structural connectivity matrix of each subject was generated according to a relatively coarse-grained atlas, which contains 68 cortical areas and 14 subcortical areas [44]. The connection weights are fixed as the number of white matter streamlines between brain regions normalized by the geometric mean of their volumes and capture the strength of interactions between brain areas to some extent. The group-level structural network (Fig 1A) was then constructed by combining all subject-level structural networks using a consistency-based thresholding method [42, 45]. The generated network shows the same binary connection density as the average across subjects and approximately the same distributions of edge length and weight as each subject [42].

Utilizing the same dataset, subject-level distance matrices were obtained by calculating the Euclidean distance between centers of brain region pairs. The group-representative distance matrix (Fig 1B) used to estimate the time delays associated with interareal communication was generated by averaging all subject-level distance matrices. More detailed information about the acquisition and preprocessing steps of diffusion-weighted MRI data is presented in [27].

Our work aims to demonstrate how noise amplitude influences the effects of local stimulation from a general perspective. Therefore, we chose a simple stimulation protocol (Fig 1C). The stimulation is applied to the brain during the third second with a constant intensity of

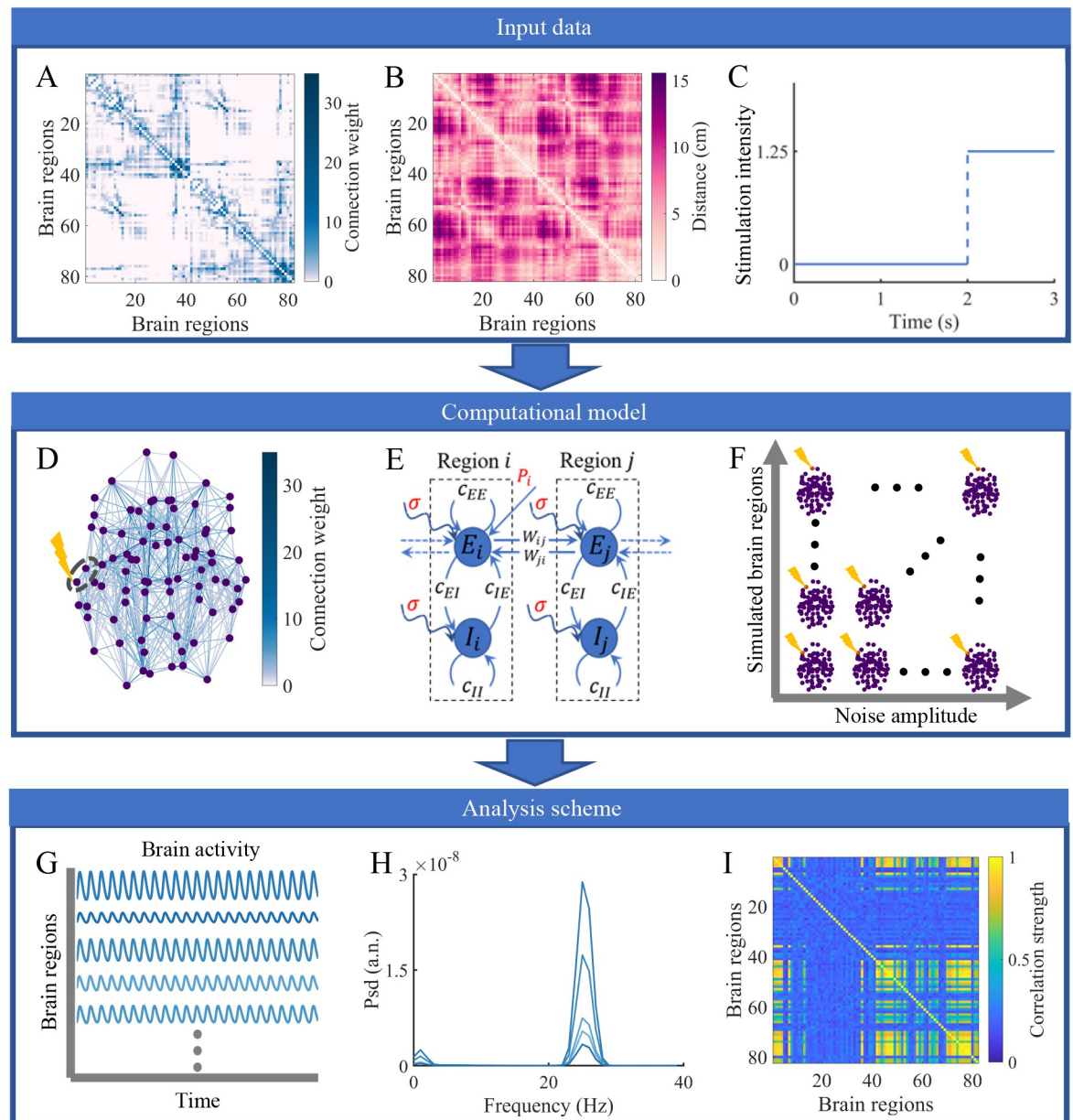


Fig 1. Workflow consisting of Input data, Computational model and Analysis scheme. (A) Group-level structural connectivity matrix based on 82-node brain parcellation. (B) Group-averaged distance matrix characterized by the same parcellation. (C) External stimulation protocol, with an intensity of 0 for the first two seconds and an intensity of 1.25 for the third second. (D) An example of local stimulation in the structural brain network. The purple dots and blue lines represent the centers of the brain regions and the strongest 20% of connections between them. The line darkness is positively related to the connection weight. The stimulated brain region indicated by the yellow lightning bolt and its unstimulated neighbor are circled to demonstrate the dynamics. (E) Schematic of two brain regions with Wilson-Cowan dynamics linked by excitatory connections. Each region includes coupled excitatory and inhibitory populations disturbed by noise with amplitude σ . An external perturbation P_i is applied to region *i* to increase the excitatory input. (F) Simulation experimental design. Different brain regions are stimulated under various noise amplitudes. (G) Time series of excitatory activity for each brain region generated by the computational model. (H) Power spectrum estimation to quantify the stimulation outcomes from a regional perspective. (I) Functional connectivity matrix used to evaluate network-level effects.

<https://doi.org/10.1371/journal.pcbi.1010866.g001>

1.25 but is absent for the first two seconds. This setting is consistent with previous theoretical research [27, 37].

Computational model

In each trial, the stimulation indicated by the yellow lightning bolt in Fig 1D is applied to a single brain region. The stimulated area and one of its neighboring areas are surrounded by a gray dotted line and their dynamics are shown in Fig 1E. To simulate brain activity, we employ a nonlinear neural mass model, which has been widely exploited to investigate brain functions [46, 47]. Each brain region is composed of both excitatory and inhibitory neural populations and is governed by the Wilson-Cowan dynamics [48]. Brain regions are coupled through the structural connectivity described above, with distance-dependent time delays. In accordance with previous works [27, 37, 49], anatomical connections link only excitatory populations in different brain areas.

The activity of the i^{th} brain region is controlled by the following equations:

$$\tau \frac{dE_i(t)}{dt} = -E_i(t) + [S_{E_{max}} - E_i(t)]S_E[c_{EE}E_i(t) - c_{IE}I_i(t) + c \sum_j A_{ij}E_j(t - \tau_{ij}) + P_i(t)] + \sigma w_i(t) \tag{1}$$

$$\tau \frac{dI_i(t)}{dt} = -I_i(t) + [S_{I_{max}} - I_i(t)]S_I[c_{EI}E_i(t) - c_{II}I_i(t)] + \sigma v_i(t) \tag{2}$$

where $E_i(t)$ and $I_i(t)$ represent the firing rates of excitatory and inhibitory pools in brain region i , and τ is a time constant for both populations. The sigmoidal transfer functions S_E and S_I of the excitatory and inhibitory populations are described by

$$S_E(x) = \frac{1}{1 + e^{(-a_E(x-\theta_E))}} - \frac{1}{1 + e^{a_E\theta_E}} \tag{3}$$

and

$$S_I(x) = \frac{1}{1 + e^{(-a_I(x-\theta_I))}} - \frac{1}{1 + e^{a_I\theta_I}}. \tag{4}$$

The fixed parameters a_E and a_I determine the maximal values of the slope, while θ_E and θ_I represent the positions of the maximum slope of the activation functions for each pool [48].

In each brain region, the excitatory pool receives local excitation from itself with strength c_{EE} , local inhibition from the inhibitory pool in the same region with strength c_{IE} , and long-range excitation from excitatory pools in other regions through group-level anatomical connectivity with connection strength A_{ij} and global coupling strength c . If region i is stimulated, its excitatory pool receives external input with strength P_i . Due to the long distance between brain areas and the limited transmission speed, we also consider the time delay between regions i and j as τ_{ij} , which is given by $\frac{D_{ij}}{v}$. D_{ij} indicates the group-representative Euclidean distance between regions i and j and v is the velocity of signal conduction. The inhibitory pool receives only local excitation from the excitatory pool in the same region with strength c_{EI} and local inhibition from itself with strength c_{II} . In addition, the excitatory and inhibitory populations are disturbed by Gaussian noise $\sigma w_i(t)$ and $\sigma v_i(t)$. The probability density functions of $w_i(t)$ and $v_i(t)$ follow standard Gaussian distributions. σ scales the standard deviations of noise realizations and is set as noise amplitude.

Table 1. Values of model parameters.

Parameter	Description	Value
τ	Time constant	8 ms
c_{EE}	Local excitatory-to-excitatory coupling strength	16
c_{IE}	Local inhibitory-to-excitatory coupling strength	12
c_{EI}	Local excitatory-to-inhibitory coupling strength	15
c_{II}	Local inhibitory-to-inhibitory coupling strength	3
a_E	Proportional to the excitatory maximum slope	1.3
a_I	Proportional to the inhibitory maximum slope	2
θ_E	Position of the excitatory maximum slope	4
θ_I	Position of the inhibitory maximum slope	3.7
$\mathcal{S}_{E_{max}}$	Maximum of the excitatory activity function	0.9945
$\mathcal{S}_{I_{max}}$	Maximum of the inhibitory activity function	0.9994
c	Global coupling strength	0.01–0.3
v	Velocity of signal conduction	10 m/s
P_i	External stimulation intensity	1.25
σ	Noise amplitude	$10^{-9} - 10^{-2}$

<https://doi.org/10.1371/journal.pcbi.1010866.t001>

To systematically explore the role of noise amplitude in modifying the stimulation outcomes, we perform multiple trials under different combinations of noise amplitudes and stimulation sites (Fig 1F).

Model parameters. The values of the model parameters used in this study are shown in Table 1 and are consistent with those used in previous research [37]. The local perturbation P_i is set as a persistent excitation during 2–3 s with an intensity of 1.25 for stimulated region i and 0 for other areas. For an isolated brain area with the parameters shown in Table 1, external stimulation causes a transition from the fixed point to the limit cycle regime [27, 37, 50]. The frequency of rhythmic activity for the stimulated region is approximately 20 Hz, which is essential in oscillatory neuronal dynamics [51, 52]. By tuning the strength of the excitatory input from other regions in the brain network, the global coupling strength c can affect the system state, as reflected in the sudden increase in the mean firing rates of most regions, indicating the dynamic transition from a low-activity steady state to a high-amplitude oscillatory state [27, 37]. Note that noise amplitude σ is the parameter of interest. Therefore, we consider the global coupling strength $c \in [0.01, 0.3]$ in steps of 0.005 and the noise amplitude $\sigma \in [10^{-9}, 10^{-2}]$ in a log manner such as $10^{-9}, 2 \times 10^{-9}, \dots, 9 \times 10^{-9}, 10^{-8}, 2 \times 10^{-8}, \dots$.

Simulation details. Due to the broad range of noise amplitude σ , we integrate the set of stochastic differential equations described above using the Euler-Maruyama scheme with a sufficiently small step ($dt = 5 \times 10^{-6}$ s). We select a constant initial condition for all regions following previous work [37, 50]. The simulations are first performed for 2 seconds without stimulation under different global coupling strengths and noise amplitudes to determine the appropriate global coupling strength c . Then, we run the main simulations for 3 seconds under different noise amplitudes and stimulation sites, with the local perturbation applied for 2–3 s. We perform each simulation 30 times and discard the first second of neural activity due to the initial instability. We mainly focus on the excitatory firing rate $E_i(t)$ in each region [37, 46, 47, 49] and downsample these time series to a resolution of 1×10^{-3} s.

Analysis metrics

We use the time series of excitatory activity in the before- (1–2 s) and during-stimulation (2–3 s) periods to evaluate the impacts of local stimulation (Fig 1G). First, from a regional

perspective, one crucial effect of local stimulation is altering neural oscillations in various brain areas, which are commonly related to brain functions and behaviors [51, 52]. Thus, we evaluate the brain state based on the characteristics of the frequency domain. We subtract the corresponding mean value from each excitatory time series and apply Welch's method with a window length of 0.5 s with 50% overlap to estimate the power spectrum density of each area (Fig 1H). Unless explicitly stated, the power spectrum density shown in this paper represents the average of 30 realizations to improve the signal-to-noise ratio. The frequency at which the regional power reaches its maximum value (peak frequency) reflects the main pattern of neural oscillations [53, 54] and is the measure of interest. The peak frequency (f_{peak}) is given by

$$f_{peak} = \arg \max_f P(f), \quad (5)$$

where $P(f)$ represents the power spectrum density of a specific area. In this work, due to the general low peak frequency of brain areas before perturbation, the peak frequency of 2–3 s captures the effects of local stimulation.

Second, the dynamic information of the brain is stored not only in individual regions but also in interactions between areas. Thus, we examine the brain state from a network viewpoint based on functional connectivity (Fig 1I), which is derived by calculating the maximum normalized cross-correlation [55, 56] between time series with a time window of 1 s and a maximum lag of 250 ms. The stimulation effects are quantified as the difference in the network-level behaviors before (1–2 s) and during (2–3 s) stimulation, namely, the functional and structural effects [37]. The functional effect (fe), which indicates the influence of local brain regions on the interregional coupling configuration, is calculated as

$$fe = |FC_d - FC_b|, \quad (6)$$

where FC_d and FC_b are the functional connectivity matrices during and before stimulation, respectively, and $||$ represents the average of the absolute values of elements in the upper triangle of the matrix. Functional effects reflect the average changes in functional networks induced by stimulation. The structural effect (se), which indicates how local changes in brain activity affect the structural constraints on brain dynamics, is given by

$$se = FC_d \cdot SC - FC_b \cdot SC, \quad (7)$$

where SC is the structural connectivity matrix and \cdot indicates calculating the Pearson correlation coefficient between two matrices. Structural effects also represent the alterations in the correspondence between structural and functional connectivity.

In addition to the basic metrics, various integrated measures were used in this study to characterize the dynamic behaviors of the brain. These measures are listed in Table 2 for ease of review.

Results

The effects of the noise amplitude and global coupling strength on brain states without stimulation

To select the optimal global coupling strength c and provide prior knowledge about the brain state under different noise amplitudes σ , we perform 2-second simulations without stimulation and investigate system behaviors under various combinations of σ and c . We change σ from 10^{-9} to 10^{-2} and c from 0.01 to 0.3.

In Fig 2A, we present the time-averaged excitatory activity $\overline{E(t)}$ as a function of the global coupling strength at a single noise amplitude ($\sigma = 10^{-5}$). The results show that there exists a

Table 2. Summary of integrated measures.

Measure	Description
$\overline{E(t)}$	Time-averaged excitatory activity
$\langle \overline{E(t)} \rangle$	Time- and network-averaged excitatory activity
$\langle f_{peak} \rangle$	Network-averaged peak frequency of the excitatory activity
$\langle p_{peak} \rangle$	Network-averaged peak power of the excitatory activity
f_{sti}^{peak}	Peak frequency of stimulated brain regions
f_{unsti}^{peak}	Peak frequency of unstimulated brain regions
$\langle f_{unsti}^{peak} \rangle$	Average peak frequency of 81 unstimulated regions
$\langle f_{unsti}^{peak} \rangle_{\sigma}$	Peak frequency of one unstimulated region averaged over all noise amplitudes
$\langle fe \rangle$	Mean of the functional effects induced by stimulating regions in a single cognitive system
$std(fe)$	Standard deviation of the functional effects induced by stimulating regions in a single cognitive system
$\langle se \rangle$	Mean of the structural effects induced by stimulating regions in a single cognitive system
$std(se)$	Standard deviation of the structural effects induced by stimulating regions in a single cognitive system

<https://doi.org/10.1371/journal.pcbi.1010866.t002>

threshold of c , above which the $\overline{E(t)}$ values in most regions change sharply. Fig 2B shows how the time- and network-averaged activity $\langle \overline{E(t)} \rangle$ varies with the noise amplitude and global coupling strength. The threshold remains constant and is unrelated to the noise amplitude. We next examine the network-averaged peak frequency and peak power ($\langle f_{peak} \rangle$ and $\langle p_{peak} \rangle$).

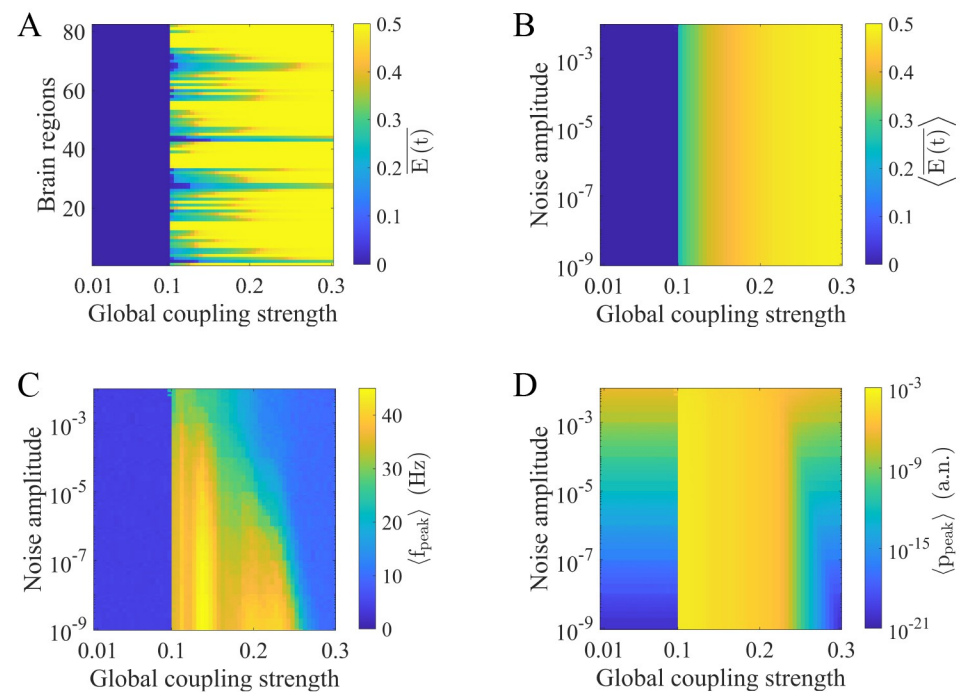


Fig 2. The effects of noise amplitude and the global coupling strength on brain states without stimulation. (A) Time-averaged excitatory activity ($\overline{E(t)}$) in each brain region under different global coupling strengths when $\sigma = 10^{-5}$. (B) Time- and network-averaged excitatory activity ($\langle \overline{E(t)} \rangle$) under different combinations of global coupling strengths and noise amplitudes. (C) Network-averaged peak frequency of the excitatory activity ($\langle f_{peak} \rangle$) under different combinations of global coupling strengths and noise amplitudes. (D) Network-averaged peak power of the excitatory activity ($\langle p_{peak} \rangle$) under different combinations of global coupling strengths and noise amplitudes.

<https://doi.org/10.1371/journal.pcbi.1010866.g002>

We find the same threshold in Fig 2C and 2D. Below this threshold, the results show that $\langle f_{peak} \rangle$ is less than 10 HZ and $\langle p_{peak} \rangle$ is relatively low. Note that a larger noise amplitude leads to a larger $\langle p_{peak} \rangle$. Moreover, slightly above the threshold, $\langle f_{peak} \rangle$ and $\langle p_{peak} \rangle$ are both considerably enhanced. Consistent with previous studies, our results indicate that crossing the threshold triggers bifurcations in most brain regions [27, 37, 41]. These systemic changes shift nodes from low-activity steady states with noise-driven fluctuations to high-amplitude oscillatory states.

Overall, Fig 2B–2D reveals that a noise-independent threshold separates the two dynamical regimes. According to previous research [37, 41], we choose the value just below the threshold as the optimal global coupling strength ($c = 0.1$). This approach aligns with the widely accepted assumption that the fluctuation regime best captures empirical brain function, providing optimal information processing flexibility [38, 57, 58]. At the chosen value, σ has little effect on $\langle E(t) \rangle$ and $\langle f_{peak} \rangle$, except for $\langle p_{peak} \rangle$. This result indicates that the noise amplitude does not produce qualitative changes in brain states, providing a relatively uniform baseline. Note that there are several high $\langle f_{peak} \rangle$ values at large σ when $c = 0.1$ in Fig 2C. This is because large noise amplitudes combined with the initial values of simulations may induce oscillations in some regions with a limited number of realizations, which has little impact on the following analyses. We also show the distributions of $\langle f_{peak} \rangle$ and $\langle p_{peak} \rangle$ in all brain regions under the chosen c and different σ in S1 and S2 Figs to provide additional information.

The regional peak frequency during stimulation depends on the interplay between the noise amplitude and structural connectivity strength

In this section, we explore the peak frequency in both stimulated and unstimulated brain regions at a global coupling strength of 0.1. We mainly focus on the following problems: How does noise amplitude affect the regional peak frequency during stimulation? Moreover, given the important role of the anatomical network in shaping neural dynamics [59], how do the noise amplitude and structural properties jointly modulate the regional peak frequency?

Fig 3A presents the peak frequencies in stimulated brain areas (f_{sti}^{peak}) as a function of the noise amplitude and stimulation site. The external perturbation drives the stimulated region to an oscillatory state, leading to higher f_{sti}^{peak} values than the case without stimulation. The results show that f_{sti}^{peak} is related to the stimulation site but is rarely affected by the noise amplitude. Note that different stimulation sites influence the transmission pathways for the altered neural activity and are assumed to reflect properties of the structural brain network.

We then consider the peak frequency in unstimulated brain regions (f_{unsti}^{peak}). Unlike stimulated areas that directly receive external perturbations, these regions are indirectly affected through interactions with other regions. Fig 3B shows the impact of the noise amplitude at a fixed stimulation site (R-Precentral). When σ is low, most regions exhibit high f_{unsti}^{peak} , indicating that these regions effectively received the activity from the stimulated area. As σ increases, more regions exhibit low f_{unsti}^{peak} values, which implies that activity transmission is hindered. The behaviors of some other stimulation sites are provided in S3 Fig to validate the robustness of our results. Fig 3C shows the average peak frequency of 81 unstimulated brain regions ($\langle f_{unsti}^{peak} \rangle$) under different combinations of stimulation sites and noise amplitudes. The results show that σ reduces $\langle f_{sti}^{peak} \rangle$ for all stimulation sites, disturbing information transmission. Note that the effects of the noise amplitude differ at various stimulation sites. Some regions are more susceptible to noise and exhibit decreased $\langle f_{unsti}^{peak} \rangle$ at relatively low σ . However, some other regions show the opposite behavior, indicating the complex interplay between the noise amplitude and network structure. Additionally, several large values at high σ can be observed

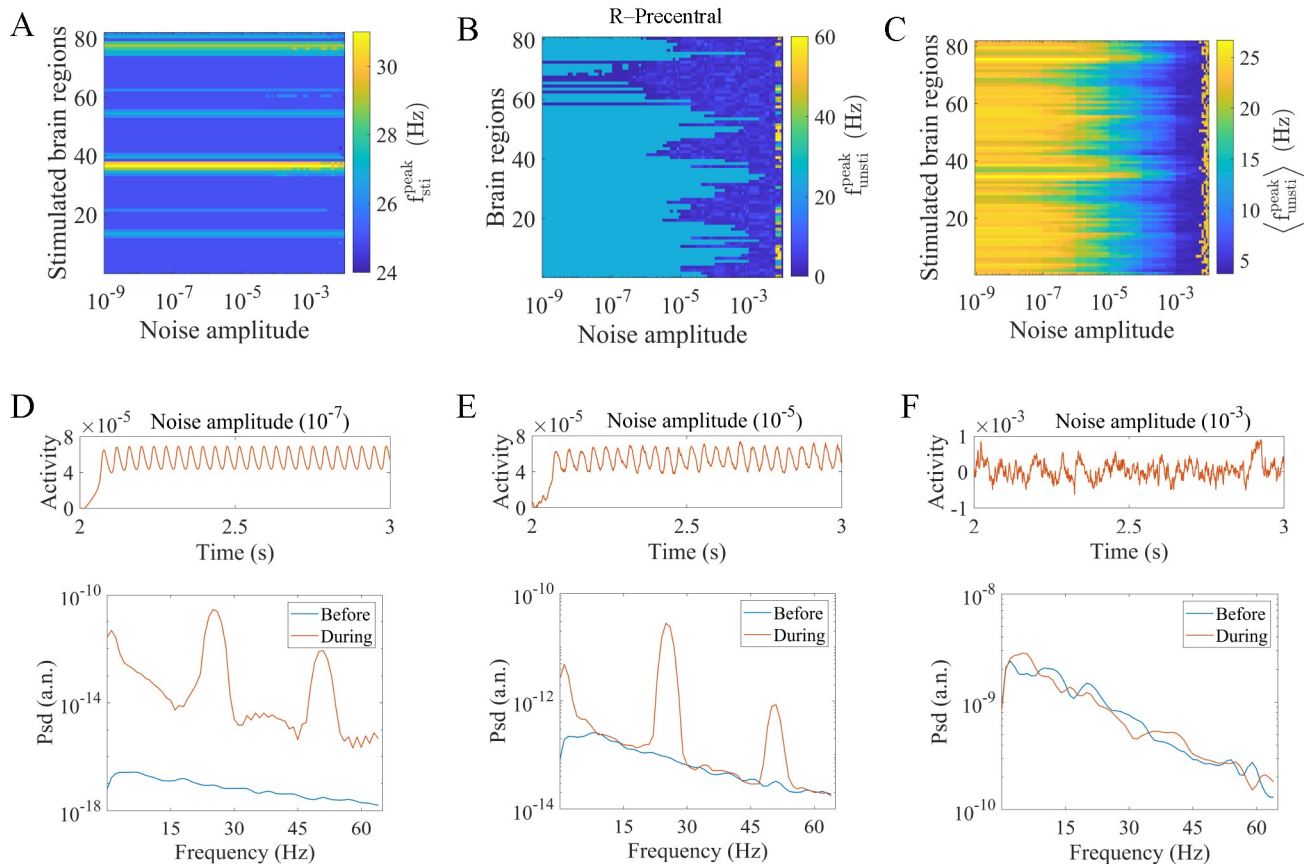


Fig 3. The effects of noise amplitude and the stimulation site on the regional peak frequency during stimulation. (A) Peak frequency of stimulated brain regions (f_{sti}^{peak}) under different combinations of noise amplitudes and stimulation sites. (B) Peak frequency of unstimulated brain regions (f_{unsti}^{peak}) as a function of the noise amplitude when stimulating R-Precentral. (C) Average peak frequency of 81 unstimulated regions ($\langle f_{unsti}^{peak} \rangle$) under different combinations of noise amplitudes and stimulation sites. (D) (E) (F) Time series (upper panels) and power spectra (lower panels) of an unstimulated region (R-Precuneus) when stimulating the R-Lateral Orbitofrontal under different noise amplitudes (10^{-7} , 10^{-5} , 10^{-3}). The blue and orange lines in the lower panels indicate the power spectrum before and during stimulation, respectively.

<https://doi.org/10.1371/journal.pcbi.1010866.g003>

in Fig 3B and 3C because the system is already in an oscillatory state before stimulation (Figs 2C and S1 Fig). We also provide examples of time series and power spectra of an oscillatory unstimulated region in S4 Fig. Results show that the local stimulation barely affects the high peak frequency during stimulation.

To further elucidate the behaviors of unstimulated brain areas, we investigate the time series and power spectra of the R-Precuneus when stimulating the R-Lateral Orbitofrontal under different noise amplitudes as typical examples (Fig 3D, 3E and 3F). We find that as the noise amplitude increases, the regional activity becomes increasingly irregular. Moreover, the power spectrum before stimulation increases and constrains that during stimulation as a lower bound. To ensure the robustness of our findings, we also present the behaviors of several unstimulated brain regions in S5 Fig.

We further explore the relationship between the noise amplitude and the network structure by investigating how oscillatory activity propagates from stimulated to unstimulated regions. In Fig 4A, 4B and 4C, we show three typical examples of f_{unsti}^{peak} matrices under fixed noise amplitudes ($\sigma = 10^{-7}$, 10^{-5} , 10^{-3}). Each element in the matrices represents the peak frequency of an unstimulated brain region (y-axis) under a specific stimulated area (x-axis). We observe that

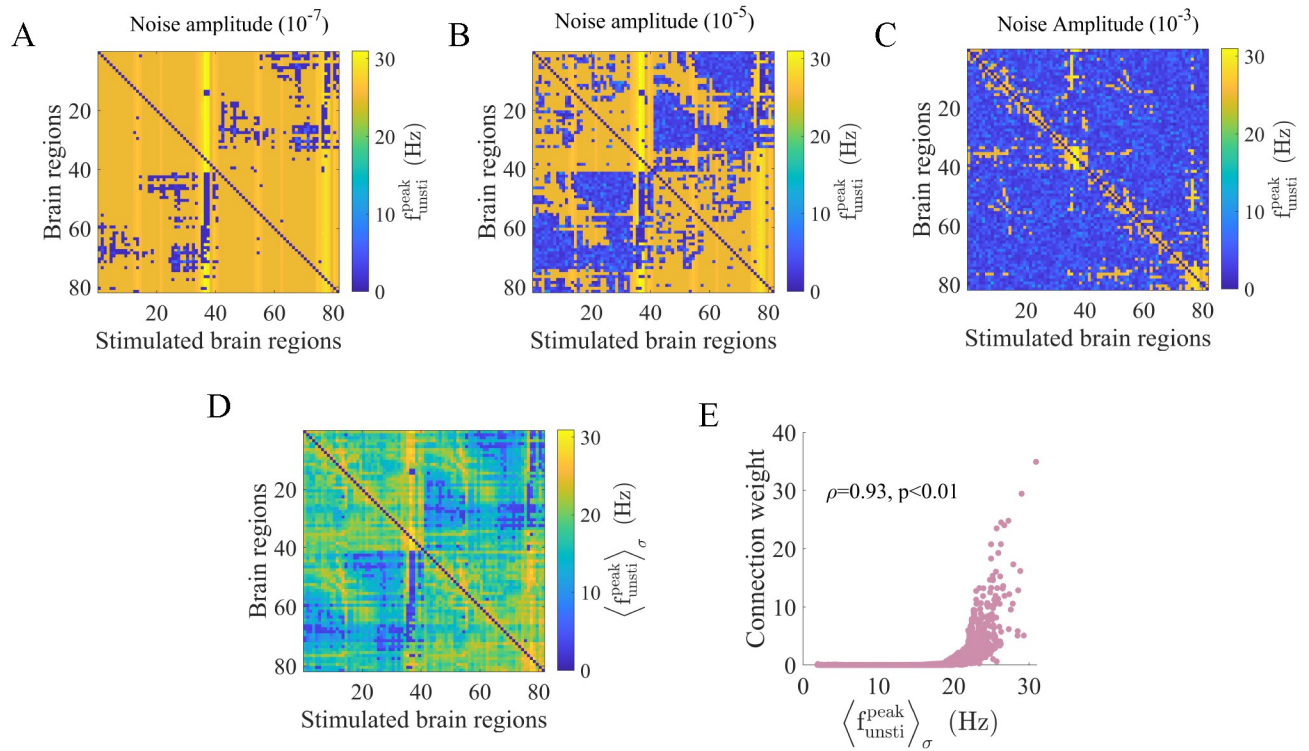


Fig 4. The high similarity between the peak frequency of unstimulated areas averaged across noise amplitudes and the structural connectivity. (A) (B) (C) The peak frequency (f_{unsti}^{peak}) of unstimulated brain regions (y-axis) under various stimulated regions (x-axis) at different noise amplitudes (10^{-7} , 10^{-5} , 10^{-3}). The diagonal elements are set to 0. (D) Peak frequency of unstimulated regions (y-axis) under different stimulation sites (x-axis) averaged across all noise amplitudes ($\langle f_{unsti}^{peak} \rangle_{\sigma}$), with the diagonal elements set to 0. (E) The positive Spearman correlation ($\rho = 0.93, p < 0.01$) between the matrix in (D) and the structural connectivity network.

<https://doi.org/10.1371/journal.pcbi.1010866.g004>

the f_{unsti}^{peak} values heterogeneously decrease as σ increases. Thus, we are interested in which node pairs are more vulnerable to noise and how this behavior relates to structural properties. Fig 4D presents the matrix of f_{unsti}^{peak} values averaged across noise amplitudes ($\langle f_{unsti}^{peak} \rangle_{\sigma}$). Intriguingly, this matrix is remarkably similar to the structural connectivity matrix, with a positive Spearman correlation coefficient $\rho = 0.93, p < 0.01$ (Fig 4E). Node pairs with strong direct connections tend to exhibit high f_{unsti}^{peak} values in a large range of σ , indicating strong activity transmission capability. This result reveals that the antagonistic effects of the structural connection strength and noise amplitude modulate activity propagation between stimulated and unstimulated areas in terms of the peak frequency. Note that this result also illustrates the rather small contribution of multistep paths due to the greater noise disturbance along the path. S6 Fig shows that oscillations before stimulation induced by large noise amplitudes have little impact on the positive correlation.

The heterogeneous impact of noise amplitude on structural degree alters network-level stimulation effects

In this section, we comprehensively investigate the network-level effects of stimulation (functional and structural effects) based on the functional connectivity matrix. Our goal is to explore how noise amplitude affects these network-level effects. Many previous studies have suggested that the structural degree of the stimulated region is an important feature for predicting and

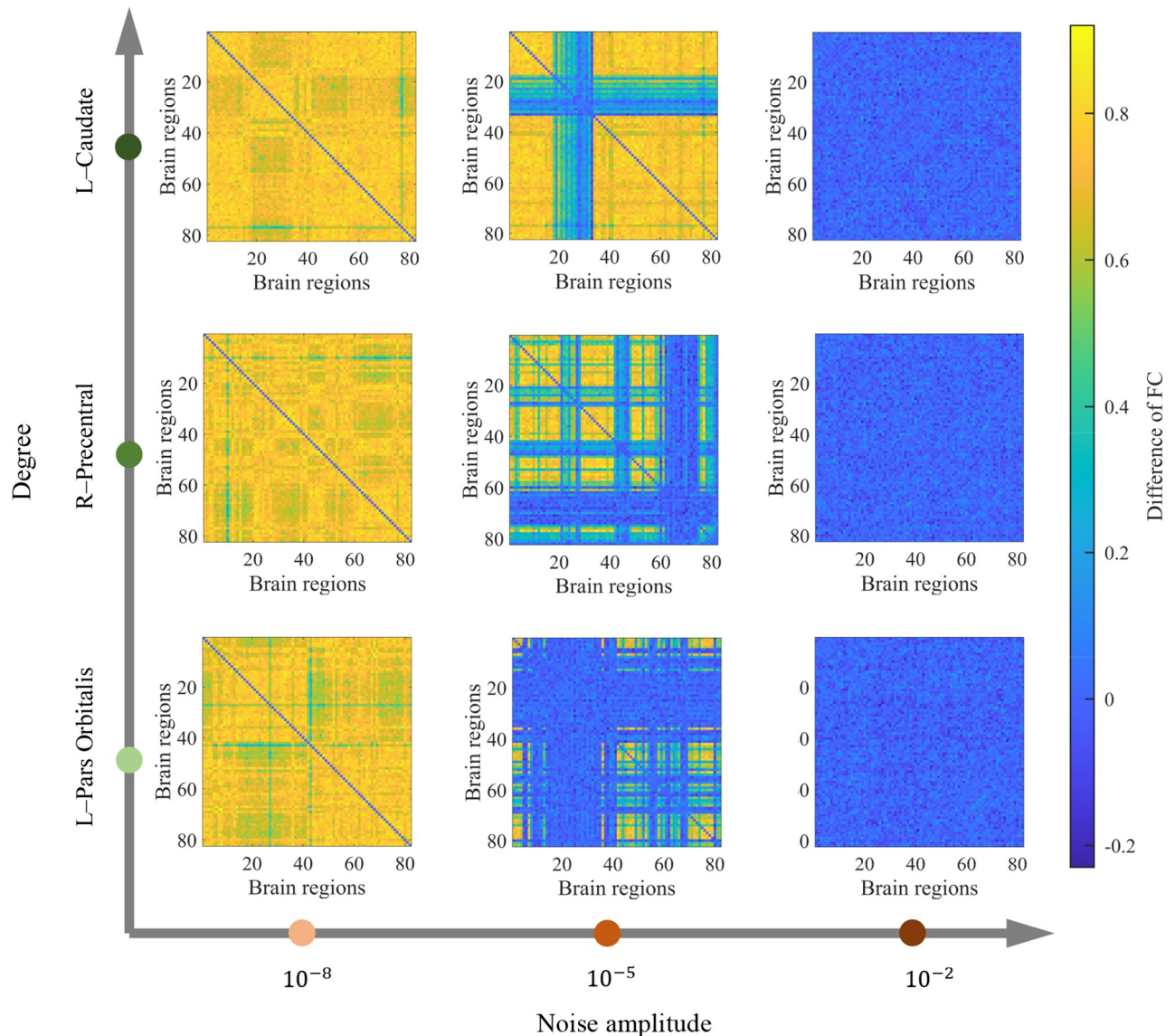


Fig 5. Examples of functional connectivity changes induced by stimulating different regions under various noise amplitudes. The brain regions L-Pars Orbitalis, R-Precentral and L-Caudate with low, moderate and high structural degrees, respectively, are stimulated at low (10^{-8}), moderate (10^{-5}) and high (10^{-2}) noise amplitudes. The matrices represent the differences in functional connectivity networks before and during local stimulation for one realization.

<https://doi.org/10.1371/journal.pcbi.1010866.g005>

controlling stimulation effects [19, 37, 60]. How does noise amplitude influence the role of the structural degree? In particular, how does noise amplitude affect the relationship between the structural degree and functional or structural effects?

Fig 5 shows the difference in functional networks before and during stimulation under three noise amplitudes ($\sigma = 10^{-8}$, 10^{-5} , 10^{-2}) at three stimulation sites with various degrees (L-Pars Orbitalis, R-Precentral and L-Caudate). We observe that as the noise amplitude increases, the changes in the functional networks decrease. When $\sigma = 10^{-8}$, most node pairs in the networks exhibit large alternations. When $\sigma = 10^{-2}$, the edge changes are small. Moreover, stimulating different regions leads to similar results in these two situations. When $\sigma = 10^{-5}$, only some node pairs are influenced. The larger the degree of the stimulated region, the larger

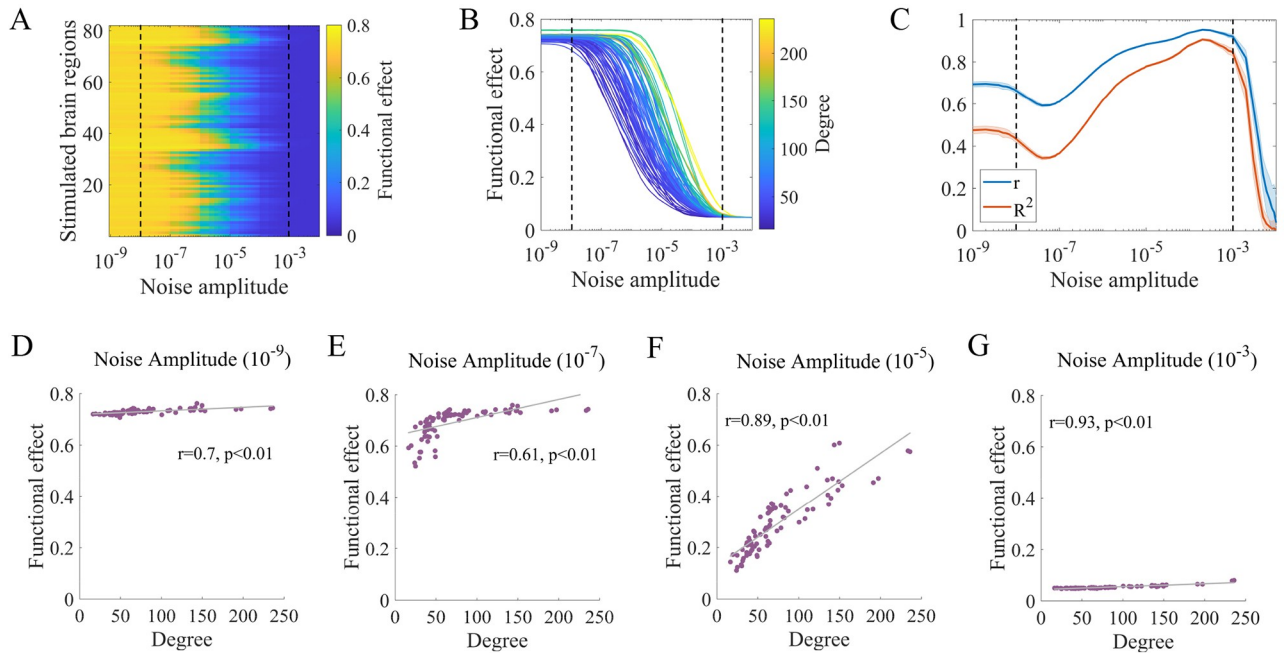


Fig 6. Noise amplitude and structural degree jointly affect the functional effects of stimulation. (A) Functional effects under different combinations of stimulation sites and noise amplitudes. (B) Functional effects as a function of noise amplitude for all stimulation sites, ranked by structural degree. Note that the values in (A) and (B) represent the ensemble averages of 30 realizations of the corresponding measures. (C) Pearson correlation coefficient (r) and adjusted coefficient of determination (R^2) between functional effects and structural degree as a function of noise amplitude. The solid lines and shaded areas describe the ensemble averages and standard deviations of 30 realizations of the corresponding measures. (D) (E) (F) (G) Snapshots of the functional effects under different noise amplitudes for one realization. (D) Noise amplitude = 10^{-9} , Pearson's $r = 0.7$, $p < 0.01$. (E) Noise amplitude = 10^{-7} , Pearson's $r = 0.61$, $p < 0.01$. (F) Noise amplitude = 10^{-5} , Pearson's $r = 0.89$, $p < 0.01$. (G) Noise amplitude = 10^{-3} , Pearson's $r = 0.93$, $p < 0.01$. The gray lines represent the linear fits of data points estimated by ordinary least squares. FDR correction was performed for p-values across all noise amplitudes and realizations.

<https://doi.org/10.1371/journal.pcbi.1010866.g006>

the range of alterations in the functional network. These results provide an intuitive illustration of how noise amplitude and structural degree collectively affect network-level effects. The functional connectivity changes induced under some other stimulation sites and noise amplitudes are provided in [S7 Fig](#) to validate the robustness of the trend. We also provide examples of stimulating the brain in the oscillatory state, as shown in [S8 Fig](#).

In [Fig 6](#), we use the functional effects to quantitatively investigate how functional brain networks are affected by external perturbations. We calculate the mean of the absolute values of the upper triangular elements in the functional connectivity difference matrices induced by local stimulation. [Fig 6A](#) shows the functional effects under different combinations of noise amplitudes and stimulation sites. The impact of the noise amplitude can be separated into three distinct regimes. In the first regime ($\sigma < 10^{-8}$), large functional effects are independent of the noise amplitude, and the local stimulation alters the system into a state that differs considerably from the prestimulation situation. In the second regime ($10^{-8} < \sigma < 10^{-3}$), the functional effects gradually decrease as σ increases, showing disturbance effects. In the third regime ($\sigma > 10^{-3}$), the functional effects are approximately 0, and the local stimulation has little impact on the brain. Moreover, there is obvious heterogeneity among stimulation sites under specific noise amplitudes, especially in the second regime, indicating the effect of brain structure. Additionally, note that the stimulation sites exhibit different levels of resistance to noise. To understand the role of the structural degree and its interaction with the noise amplitudes, we exhibit the functional effects versus the noise amplitude separately for each stimulation site and color the effects according to the corresponding degree, as shown in [Fig 6B](#). We found

that the larger the degree of the stimulation site, the larger the functional effects under a fixed noise amplitude and the stronger the noise amplitude required to reduce functional effects. This result demonstrates the heterogeneous effect of noise on the degree, i.e., regions with large degrees not only have a high capacity to influence brain dynamics but also show strong resistance to noise.

In Fig 6C, the Pearson correlation coefficient r between the functional effects and structural degree as well as the adjusted coefficient of determination R^2 estimated via an ordinary least squares method are presented as functions of the noise amplitude. High absolute values of r and R^2 indicate that the functional effects are highly linearly correlated with and well fitted by the corresponding degree. FDR-corrected p-values of Pearson correlation coefficients for all realizations are shown in S9 Fig to provide statistical significance across noise amplitudes. The results show that noise amplitude nonmonotonically modulates the relationship between functional effects and structural degree. Initially, r shows intermediate values and remains approximately constant (first regime); r then decreases to a local minimum and increases to a global maximum (second regime); finally, r rapidly declines to 0 (third regime). R^2 shows a similar trend. We also provide typical snapshots of the functional effects under different noise amplitudes in Fig 6D–6G ($\sigma = 10^{-9}, 10^{-7}, 10^{-5}, 10^{-3}$). Snapshots under other noise amplitudes are shown in S10 Fig. When $\sigma = 10^{-5}$, we observe a high positive association for functional effects (Fig 6F), which is consistent with a previous study [37]. However, only a moderate level of correlation was observed when the noise had little impact on brain dynamics (Fig 6D), indicating its nontrivial role. Furthermore, increasing the noise amplitude in the second regime could progressively enhance the correlation and the predictability of functional effects (Fig 6C and 6E–6G).

To better understand these behaviors, we provide further explanations from the perspective of the underlying dynamical mechanisms. In general, functional effects depend on the interplay between network structure and noise amplitude. Under the small noise amplitude which has little impact on neural activity (Fig 6D), the intrinsic network structure plays a major role. Stimulation sites with larger degrees tend to have more neighbors with higher connection weights and shorter transmission delays than regions with smaller degrees [61], thereby facilitating more effective information transmission. Therefore, although the functional effects are all quite high, they are moderately correlated with the structural degree. Stimulation sites with small degrees limit information transmission, causing the propagation of downstream activity sensitive to the increased noise amplitude. When the noise amplitude is slightly larger (Fig 6E), the functional effects induced by stimulation to small-degree regions are reduced, while the functional effects are essentially unchanged for regions with large degrees. This relationship becomes nonlinear and the linearity diminishes. As the noise amplitude gradually increases (Fig 6F and 6G), the downstream activity transmission is significantly hindered. However, neighboring areas are less affected due to their direct connections with stimulated regions. This situation suggests that the structural degree plays a progressively important role in predicting the response to stimulation, leading to the linearity increasing, although the functional effects decrease.

A crucial feature of the brain is the ability to support complex dynamic functions through a relatively static network structure. Therefore, the structure-function coupling can reflect the network-level state. In Fig 7, we study the alterations in the extent to which brain function is constrained by the network structure through structural effects. We calculate the difference in the Pearson correlation coefficient between the structural and functional connectivity matrices before and during stimulation. Fig 7A exhibits the structural effects as a function of the noise amplitude and stimulation site. We evaluate the structural effects according to the three regimes shown in Fig 6. In the first regime, the structural effects show moderate values and are

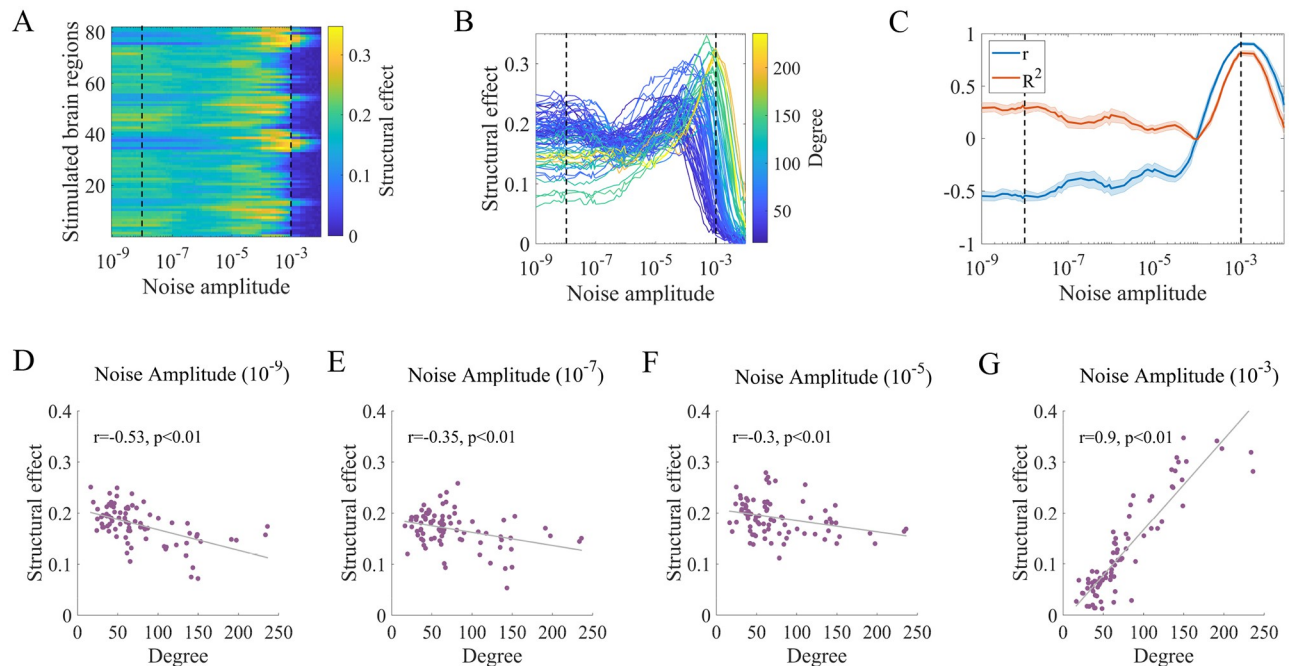


Fig 7. Noise amplitude and structural degree jointly influence the structural effects of stimulation. (A) Structural effects under different combinations of stimulation sites and noise amplitudes. (B) Structural effects as a function of noise amplitude for all stimulation sites, ranked by structural degree. Note that the values in (A) and (B) represent the ensemble averages of 30 realizations of corresponding measures. (C) Pearson correlation coefficient (r) and adjusted coefficient of determination (R^2) between structural effects and structural degree as a function of the noise amplitude. The solid lines and shaded areas describe the ensemble averages and standard deviations of 30 realizations of corresponding measures. (D) (E) (F) (G) Snapshots of structural effects under different noise amplitudes for one realization. (D) Noise amplitude = 10^{-9} , Pearson's $r = -0.53$, $p < 0.01$. (E) Noise amplitude = 10^{-7} , Pearson's $r = -0.35$, $p < 0.01$. (F) Noise amplitude = 10^{-5} , Pearson's $r = -0.3$, $p < 0.01$. (G) Noise amplitude = 10^{-3} , Pearson's $r = 0.9$, $p < 0.01$. The gray lines represent the linear fits of data points estimated by ordinary least squares. FDR correction was performed for p-values across all noise amplitudes and realizations.

<https://doi.org/10.1371/journal.pcbi.1010866.g007>

independent of the noise amplitude. Local stimulation causes a temperate increase in the similarity between the structural and functional connectivity. In the second regime, the structural effects of each region increase to their peak values under large noise amplitudes, indicating that functional connectivity is more constrained by the network structure. In the third regime, all structural effects decrease to small values near 0. Moreover, we observe heterogeneous behaviors among stimulation sites, especially in the second regime, indicating the crucial role of the interaction between noise amplitude and network structure. Following previous analyses, we present the structural effects as a function of the noise amplitude separately for all stimulation sites and color the results according to the corresponding degree, as shown in Fig 7B. We find that the structural degree is not only related to the structural effects under a fixed noise amplitude but also positively correlated with the noise amplitude required to achieve the peak values in the second regime. This result indicates that the noise amplitude has a diverse influence on the degree, leading to the various performance of structural constraints across stimulated regions.

Analogous to Fig 6C, we show the Pearson correlation coefficient r and the adjusted coefficient of determination R^2 for the structural effects in Fig 7C. FDR-corrected p-values of Pearson correlation coefficients for all realizations are shown in S11 Fig to provide statistical significance. The association between the structural effects and structural degree is nonmonotonically affected by the noise amplitude. In the first regime, r and R^2 exhibit moderate values with opposite signs. In the second regime, r remains negative and then rapidly increases to a

positive value near 1. R^2 shows similar behavior but with positive values. In the third regime, both metrics rapidly decrease. Typical snapshots of the structural effects under different noise amplitudes are shown in Fig 7D–7G ($\sigma = 10^{-9}, 10^{-7}, 10^{-5}, 10^{-3}$). Snapshots under other noise amplitudes are illustrated in S12 Fig. When $\sigma = 10^{-5}$, we find a weak negative association for the structural effects (Fig 7F), which is consistent with a previous study showing poor predictability [37]. Nevertheless, our results indicate that when the noise amplitude is larger, the structural effects are highly correlated with and well predicted by the structural degree (Fig 7G). Specifically, increasing the noise amplitude in the second regime can enhance the structural effect correlations and even change its sign from negative to positive (Fig 7C and 7E–7G).

To better understand these changes, we offer interpretations based on fundamental dynamical mechanisms. The structural effects reflect the similarity between structural and functional connectivity, which is modulated by the stimulation site and noise amplitude. Under relatively low noise amplitudes (Fig 7D–7F), stimulating regions with large degrees produces high functional connectivity in most node pairs, indicating the low correspondence between the structural and functional connectivity and the reduced structural effects. In contrast, stimulating regions with small degrees leads to more node pairs showing low functional connectivity. As the structural connection weights reflect the information transmission ability to some extent, the low functional connectivity is more likely to be found at node pairs with low connection weights, therefore inducing higher structural constraints. Consequently, the structural effects are negatively correlated with the structural degree. As the noise amplitude increases (Fig 7G), disturbance effects are enhanced. Most functional connectivity shows values near 0 when stimulating small-degree areas, indicating the low correspondence between the structural and functional connectivity and reduced structural effects. For large-degree stimulation sites, more functional connectivity shows high values, which is more likely to be found at node pairs with high structural connection weights, resulting in high structural constraints. Hence, the structural effects are positively correlated with the structural degree.

Behaviors of cognitive systems in the structure-function landscape are jointly modulated by noise amplitude and the average system degree

In this section, we categorize brain regions according to cognitive systems, stimulate areas within each system, and study system behaviors based on local stimulation effects. We employ a coarse-grained classification with four cognitive systems: the sensory and association (SA) system, higher-order cognitive (HOC) system, medial default mode (MDM) system and subcortical system [62]. The stimulation effects are evaluated according to the functional and structural effects. Previous research has shown that the cognitive functions of brain systems are related to their stimulation effects [37, 50]. Here, we focus on the following questions: How does noise amplitude influence the stimulation effects of different cognitive systems? What is the association between noise-induced impacts and the system-level network structure?

In Fig 8A and 8B, we present the mean and standard deviation of the functional effects induced by stimulating regions in single cognitive systems ($\langle fe \rangle$ and $std(fe)$) as a function of the noise amplitude. Fig 8A shows that $\langle fe \rangle$ of each system nonlinearly decreases as the noise amplitude increases. The subcortical system shows the highest noise amplitude required to reduce $\langle fe \rangle$, followed by the MDM, HOC and SA systems. Moreover, the $\langle fe \rangle$ of different cognitive systems follow the same order at various noise amplitudes, indicating a relatively consistent pattern in terms of the impacts on the functional configuration. According to Fig 8B, as the noise amplitude increases, $std(fe)$ first increases to a global maximum and then decreases to 0. The SA system is the first to reach its peak value, followed by the HOC and MDM

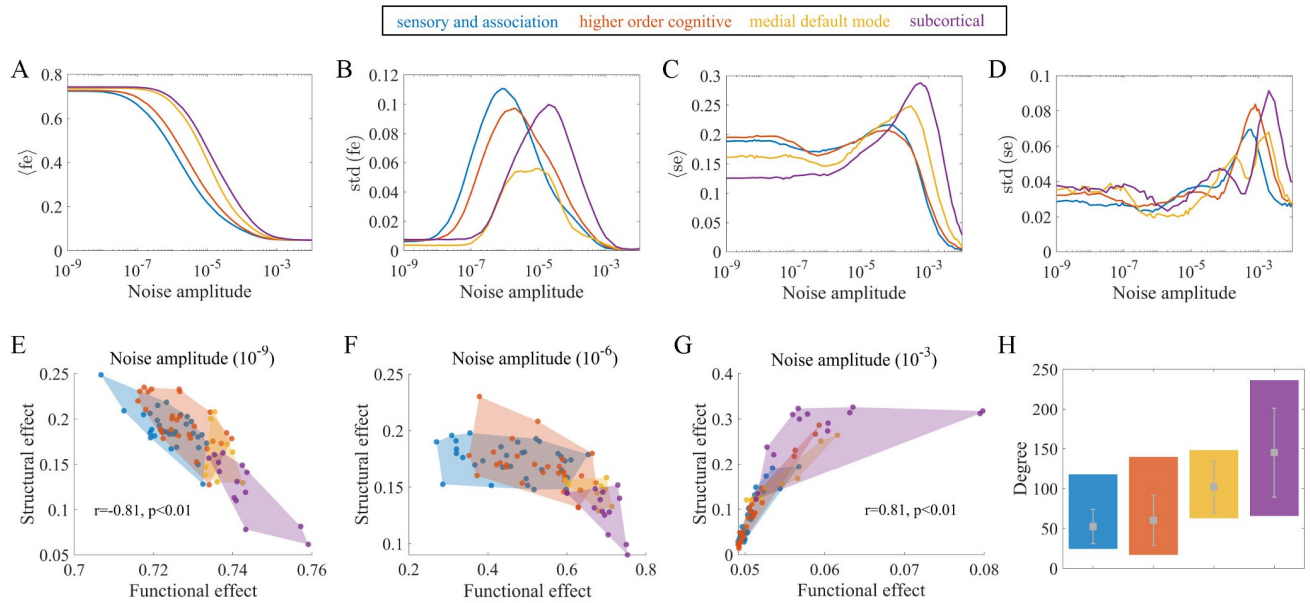


Fig 8. The associations between behaviors of cognitive systems and noise amplitude and the average system degree. (A) Mean of the functional effects induced by stimulating regions in a single system ($\langle fe \rangle$) versus the noise amplitude. (B) Standard deviation of the functional effects induced by stimulating regions in a single system ($std(fe)$) versus the noise amplitude. (C) Mean of the structural effects induced by stimulating regions in a single system ($\langle se \rangle$) versus the noise amplitude. (D) Standard deviation of the structural effects induced by stimulating regions in a single system ($std(se)$) versus the noise amplitude. (E) (F) (G) Structural effects versus functional effects of cognitive systems at various noise amplitudes (10^{-9} , 10^{-6} , 10^{-3}). Note that the brain regions are grouped into 4 cognitive systems, as indicated by the different colors. The colored areas represent the convex hulls of data points in the systems. The lines and points reflect the measures averaged over 30 realizations. (H) Structural properties of each cognitive system. The colored bars indicate the maximum and minimum structural degree of regions in the systems. The gray dots and error bars represent the mean and standard deviation of the structural degree in the systems.

<https://doi.org/10.1371/journal.pcbi.1010866.g008>

systems, and finally, the subcortical system, indicating the different levels of flexibility of functional effects in distinct systems at various noise amplitudes.

Fig 8C and 8D shows the mean and standard deviation of the structural effects in each cognitive system ($\langle se \rangle$ and $std(se)$). Fig 8C presents that as the noise amplitude increases, $\langle se \rangle$ initially shows a moderate value, then increases to a maximum and finally decreases. The noise amplitude corresponding to the peak value of $\langle se \rangle$ in the subcortical system is larger than that in the SA and HOC systems, while the MDM system shows a moderate value. The $\langle se \rangle$ of the different systems under large noise amplitudes follow the same order. Nevertheless, the opposite trend was observed under small noise amplitudes, with the SA and HOC systems showing the largest $\langle se \rangle$, indicating the altered profiles of cognitive systems at various noise amplitudes in terms of structural constraints. The $std(se)$ shows similar trends to $\langle se \rangle$ with global peaks, as presented in Fig 8D. The SA and HOC systems reach their global maximums at lower noise amplitudes than the MDM and subcortical systems, leading to different expressions of the variability of structural constraints across noise amplitudes.

Fig 8E–8G presents the locations of cognitive systems in the structure-function landscape under different noise amplitudes ($\sigma = 10^{-9}$, 10^{-6} , 10^{-3}). According to Fig 8E, the functional effects are negatively related to the structural effects. In contrast to the other systems, regions in the SA and HOC systems have smaller impacts on functional configurations and are more constrained by the structural network, while stimulating subcortical areas shows the opposite behavior. Fig 8F shows the nonlinear relationship between functional and structural effects, which is comparable to the inverted U-shaped curve discussed in previous research [37]. Stimulating regions in the SA and HOC systems results in high variability of functional effects

which are highly constrained by the structural network. In contrast, regions in the MDM and subcortical systems exhibit large functional effects and small structural effects. Fig 8G shows a positive association between these two measures. Stimulating subcortical areas are more structurally constrained than the SA and HOC systems. Overall, these results indicate that the noise amplitude not only alters the stimulation effects of different cognitive systems but also their relations with each other. The locations of different cognitive systems under other noise amplitudes are shown in S13 Fig.

Finally, we present the properties of the structural degree of each cognitive system in Fig 8H. We observe that the subcortical system has the highest average degree, followed by the MDM, HOC and SA systems. This order is consistent with many cognitive system ranks of noise-related stimulation effects, such as values and resistance to noise in Fig 8A, the values in Fig 8C and the noise amplitude corresponding to the peak values in Fig 8B–8D. These results highlight the mechanism of the mean structural degree as an intrinsic property of cognitive systems in modulating noise-related effects and indicate that the normal function of cognitive systems is jointly dependent on the noise amplitude and network structure.

Discussion

Understanding the effects of local stimulation is essential for revealing the causal relationship between neural activity and cognition and promoting clinical applications for regulating or restoring brain function [10–16]. Although many efforts have been made in exploring fundamental principles, the global response to stimulation is not fully understood. Given the evidence that noise contributes to the variability across subjects and that the modulation of neural activity induced by noninvasive stimulation may alter the signal-noise relationship [35, 36], we hypothesize that noise amplitude is a crucial factor affecting neural activity patterns during stimulation.

Inspired by past theoretical work [27, 37, 38, 40], we used a whole-brain biophysical model to simulate neural activity under different combinations of noise amplitudes and stimulation sites. We aimed to elucidate the associations between noise amplitude and the impacts of local stimulation and, more importantly, the interplay between noise amplitude and network structure. We first determined an optimal value for the global coupling strength before stimulation and then assessed the effects of regional perturbations. From a regional perspective, local perturbations increased the peak frequency of neural activity, similar to previous findings in natural and experimental stimulation studies [36, 63]. We observed that noise amplitude has little impact on the peak frequency of stimulated brain regions but reduced that of unstimulated areas. In addition, we found a high similarity between the peak frequency matrix for unstimulated areas averaged across various noise amplitudes and the structural network. From a network perspective, we quantified the effects of stimulation by examining the overall changes in functional connectivity (functional effects) and the variations in structure–function coupling (structural effects). We observed that noise amplitude nonlinearly decreased functional effects and nonmonotonically modulated structural effects. Crucially, we found that noise amplitude could enhance both the Pearson correlation coefficient and adjusted coefficient of determination between the structural degree and functional and structural effects, which has potential utility in predicting and controlling therapeutic performance. Finally, we showed that the behaviors of different cognitive systems in the landscape of functional and structural effects depended on the interplay between the noise amplitude and system-level average structural degree.

We first provide a discussion on the impacts of noise amplitude. Noise is inevitable and common in the brain and shows both detrimental effects and potential benefits [28, 64]. We

showed that under small noise amplitudes, the altered activity pattern of the stimulated area could spread throughout the network, resulting in high peak frequencies in most brain areas and strong functional couplings between areas. This behavior is an abnormal manifestation resembling the state induced by generalized epilepsy, which is often associated with enhanced interregional synchronization and is not conducive to effective information processing [65, 66]. In contrast, large noise amplitudes disrupted the transmission of neural activity; most regional peak frequencies and functional couplings could not be enhanced by local stimulation. Previous research has shown that many brain disorders such as autism, schizophrenia and cognitive dysfunction induced by aging or fibromyalgia are linked to increased neural noise [67–71]. These decreased signal-to-noise ratios have been shown to contribute to power spectrum density changes, decreased oscillatory coherence and network communication errors [72], similar to our findings. Furthermore, stimulation under moderate noise amplitudes tends to cause mild effects, with only part of the brain being affected. This result is consistent with a previous study on the chimera state, emphasizing the importance of the partial synchronization state in cognition [50]. These findings indicate that neural noise amplitude may be crucial in affecting widespread changes in regional activity and functional interactions caused by stimulation. Our results augment the literature on how noise affects neural communication dynamics from the perspective of local stimulation. Our results also support the notion that an appropriate noise amplitude is essential for maintaining brain functions such as receiving external environmental stimuli, performing internal information processing and executing normal cognitive functions [29–34, 73, 74].

Our analyses also demonstrated that noise amplitude nonmonotonically modulates the dependence of brain function on structure, i.e., structural effects. This finding is reminiscent of a recent study showing that changes in neural noise in some brain regions drive structure-function decoupling [75]. In particular, we showed that increasing the noise amplitude in the second regime could improve the correspondence between structural and functional connectivity induced by stimulation. This result reflects the complex behaviors associated with the structure-function relationship and may be relevant to normative brain dynamics [76].

The critical role of noise amplitude in neural dynamics during stimulation shows potential implications for future studies and clinical applications. These results may contribute to a deeper understanding of the highly variable consequences of brain stimulation [26] by considering the individual differences in noise amplitude. Our results could also facilitate the development of personalized stimulation protocols [25]. In particular, for patients with brain disorders characterized by abnormal neural noise, such as autism and schizophrenia [67–69], local stimulation is commonly utilized as a treatment technique. Therapists should carefully consider the function of noise amplitude and finely adjust the stimulation protocol to achieve the desired effect.

Recent studies have suggested that ketamine anesthesia increases the randomness of neural activity and likely reduces the neural signal-to-noise ratio [77, 78]. Furthermore, the effects of ketamine vary across brain regions [79, 80], resulting in different stimulation impacts. For example, stimulation to the ventral tegmental area under ketamine anesthesia elicits smaller network activation than in the awake state [81]. In contrast, stimulation to the parietal cortex shows similar distal effects in both states [82]. Analogously, in this work, we found a heterogeneous effect of noise amplitude on stimulation sites in terms of both regional and network-level stimulation effects. Here, we conceptualize stimulation sites as structural network properties and discuss the interaction between the noise amplitude and network structure.

From a regional perspective, the positive correlation between the peak frequency of unstimulated areas under different stimulation sites averaged across noise amplitudes and the structural connectivity implies an antagonistic effect between structural connection strength and

noise amplitude. The gradually increasing noise amplitude acts as a high-pass filter on the structural brain network and is more likely to impede communication between node pairs with weak weights. The relationship between brain structure and function is one of the most important challenges in neuroscience [83]. Many studies have focused on predicting brain function according to network structure [84–87]. In this work, by leveraging noise amplitude and local perturbations, we could derive information about the structural network based on the functional data obtained from numerical simulations, which improves our understanding of structure-function associations in the brain.

It is of great interest to predict and control network-level responses to stimulation [10, 88], and many studies have proposed the structural degree as an important property [19, 60]. We observed that under a moderate noise amplitude (10^{-5}), the structural degree showed a strong positive correlation with functional effects and a weak negative correlation with structural effects. This result is in accordance with a previous study showing that the structural degree mainly controls functional effects and that structural effects could not be easily predicted based on whether an area was a hub or nonhub [37]. Furthermore, we found that the noise amplitude modulates the association between the structural degree with functional and structural effects in a nontrivial way. In particular, there was only a moderate level of correlation when the noise amplitude had little impact on brain dynamics. Thus, the fact that the structural degree could serve as a good predictor of functional effects is not only an intrinsic property of the network structure but also attributed to the noise amplitude. This result deepens our understanding of the structural degree and emphasizes the significance of considering specific dynamical processes when investigating the role of structure [89]. Our results also indicate that increasing the noise amplitude within specific ranges of the second regime improves the association for functional and structural effects. The growing noise amplitude even influences the sign of the correlation for structural effects, changing it from negative to positive. These findings shed light on the fundamental action mechanisms of local stimulation and highlight the importance of coupling multiple neurophysiological factors, including brain structure and noise amplitude. A recent study supports this notion by showing that both stimulation sites and brain collective oscillatory states can alter the widespread impacts of focal stimulation [27]. Considering the coupling of other or more factors in the future is a feasible direction for fully understanding the overall effect of stimulation.

The combined effects between noise amplitude and network structure show potential clinical applications. In particular, by artificially adjusting the noise amplitude, the improved correlation offer possibilities to better predict and control stimulation effects [90, 91] based on structural connectivity networks. Note that there is a trade-off between functional effects and their predictability (Fig 6B and 6C). The maximum r and R^2 values are achieved under large noise amplitudes at the expense of functional effects. In this case, local stimulation only induces a small fraction of changes in functional networks, regardless of the stimulation site. In contrast, at lower noise amplitudes, local perturbations produce broad changes in functional connectivity. However, the r and R^2 values are reduced to some extent. This trade-off suggests that therapists should carefully tune the noise amplitude according to practical needs to balance the range of impact and predictability.

Previous research has shown that brain regions exhibit specific trade-offs between functional and structural effects that are linked to their cognitive function [92, 93]. As a result, cognitive systems, which are defined as subgraphs of the brain, occupy various locations in the structure-function landscape [37, 50]. At a moderate noise amplitude (10^{-6}), we observed that the nonlinear associations between the functional and structural effects of different systems were consistent with the findings reported in [37]. Our results further showed that noise amplitude remarkably influenced the average and variability of functional and structural

effects of each cognitive system. Moreover, noise amplitude changes could alter the positions of the systems in the structure-function landscape, which may imply functional disorders. Abnormalities in the functional connectivity in the default mode and somatomotor networks and their variability have been found in schizophrenia and autism [94–96], disorders characterized by abnormal neural noise. These abnormalities are associated with motor and cognitive dysfunction. Furthermore, we observed that cognitive systems express specific organizing principles at various noise amplitudes. Taking the average functional effect as an example, the subcortical system showed the highest value and the strongest resistance to noise, while the sensory and association system exhibited the opposite trend. This result may be explained by the fact that the subcortical system tends to play a global role in network dynamics, facilitating communication between brain areas, whereas the sensory and association system tends to play a specialized role, working in segregation and activating only a small part of the brain [50, 97, 98]. These heterogeneous behaviors at various noise amplitudes were largely attributed to the system-level mean structural degree, which again emphasizes the important role of both noise amplitude and network structure in shaping brain dynamics during stimulation.

Finally, we provide several limitations of the present study and prospects for future work. Following previous studies [27], we used a structural brain network consisting of 82 areas based on a low-resolution atlas. Although the relatively small number of nodes and connections is beneficial for computationally dense simulations of key variables, this approach may ignore important structural information at finer scales. Moreover, the group-representative connectome precludes the exploration of network differences across individuals. The main goal of this work is to demonstrate from a general perspective how noise amplitude influences the effects of local stimulation. Therefore, we chose the canonical Wilson-Cowan neural mass with a constant excitation stimulation for brain dynamics. We configured the global coupling strength such that the neural activity lies just before the high-activity oscillatory state, which is assumed to support empirical brain functions and provides maximal flexibility to perturbations [38, 57, 58]. However, this computational model is a simplification of the empirical situation and thus cannot perfectly describe the patterns of neural activity [99]. Future work could consider more realistic improvements, such as incorporating complex stimulation protocols [100], additional regional heterogeneity [101–103], synaptic plasticity [104] and evolutionary development [105]. Notably, the results need to be tested experimentally using local stimulation under different noise levels to ensure biological validity. Future studies may use psychedelics such as ketamine and LSD to enhance entropy in the brain, leading to more disordered states and changes in neural noise [106]. When comparing stimulation effects under the psychedelic state to the placebo state, researchers should cautiously exclude effects other than altered neural noise caused by psychedelics. Moreover, our study could be viewed as an extension of the state-dependent stimulation, with noise amplitude reflecting brain states. In the future, the intrinsic activity of other states, such as sleep and working memory, can be considered to investigate how these states affect the stimulation outcomes.

Supporting information

S1 Fig. Distributions of the peak frequency of excitatory activity in all brain regions under different noise amplitudes given that $c = 0.1$. (A) Noise amplitude = 10^{-7} . (B) Noise amplitude = 10^{-5} . (C) Noise amplitude = 10^{-3} . (D) Noise amplitude = 10^{-2} . Panels (A–C) show similar distributions, remarkably different from that of panel (D). These results are comparable to Fig 2C.

(JPG)

S2 Fig. Distributions of the peak power of excitatory activity in all brain regions under different noise amplitudes given that $c = 0.1$. (A) Noise amplitude = 10^{-7} . (B) Noise amplitude = 10^{-5} . (C) Noise amplitude = 10^{-3} . (D) Noise amplitude = 10^{-2} . Noise amplitude increases the peak power in all brain regions, consistent with the results in Fig 2D. (JPG)

S3 Fig. Effects of noise amplitude (x-axis) on the peak frequency of unstimulated brain regions f_{unsti}^{peak} (y-axis) at various stimulation sites. (A) L-Pars Orbitalis (small degree). (B) R-Superior Frontal (moderate degree). (C) L-Caudate (large degree). (JPG)

S4 Fig. Examples of time series and power spectra of an oscillatory brain region before and during stimulation. In this realization, the unstimulated region R-Superior Parietal is already in the oscillatory state before stimulation. Results show that the high peak frequency is almost unaffected by stimulation. The upper panels of subfigures show the time series of the R-Superior Parietal region when stimulating the L-Pars Orbitalis region under a large noise amplitude (10^{-2}). The lower panels of subfigures show the power spectra of the corresponding time series. (A) Before stimulation. (B) During stimulation. (JPG)

S5 Fig. Impact of local perturbations on the time series and power spectra of different unstimulated brain regions. The upper panels of subfigures show the time series of two unstimulated brain regions at different noise amplitudes when stimulating the R-Lateral Orbitofrontal region. The lower panels of subfigures show the power spectra before (blue) and during (orange) stimulation in the corresponding condition. (A) L-Caudate, noise amplitude = 10^{-7} . (B) L-Caudate, noise amplitude = 10^{-5} . (C) L-Caudate, noise amplitude = 10^{-3} . (D) L-Pars Orbitalis, noise amplitude = 10^{-7} . (E) L-Pars Orbitalis, noise amplitude = 10^{-5} . (F) L-Pars Orbitalis, noise amplitude = 10^{-3} . (JPG)

S6 Fig. Oscillations before stimulation have little impact on the similarity between the peak frequency averaged across various noise amplitudes and the structural connectivity. (A) The peak frequency of unstimulated brain regions (f_{unsti}^{peak}) (y-axis) under different stimulated brain regions (x-axis) at a large noise amplitude (10^{-2}). The diagonal elements are set to 0. This result corresponds to oscillations before stimulation. (B) The peak frequency of unstimulated brain regions (y-axis) under different stimulation sites (x-axis) averaged across various noise amplitudes that do not induce oscillations before stimulation ($\langle f_{unsti}^{peak} \rangle_{\sigma}$). (C) The positive Spearman correlation ($\rho = 0.95$, $p < 0.01$) between the matrix in (B) and the structural network is similar to Fig 4E. (JPG)

S7 Fig. Another set of examples of functional connectivity changes induced by stimulation. Different Brain regions R-Pars Orbitalis (low degree), L-Paracentral (moderate degree) and L-Putamen (high degree) are stimulated at low (10^{-9}), moderate (10^{-4}) and high (10^{-2}) noise amplitudes. The matrices represent the differences in functional connectivity networks before and during local stimulation for one realization. (JPG)

S8 Fig. Examples of functional connectivity changes caused by stimulating different brain regions under a large noise amplitude (10^{-2}). Note that the brain is already in the oscillatory

state before stimulation for these examples. Results show small connectivity changes similar to Fig 5. (A) R-Lateral Orbitofrontal. (B) R-Hippocampus. (C) L-Accumbens. (JPG)

S9 Fig. P-values of Pearson correlation coefficients between functional effects and structural degree as a function of noise amplitude. The blue dots at each noise amplitude represent the 30 realizations of p-values. The red horizontal line indicates the position where the p-value is equal to 0.05. FDR correction was performed for p-values across all noise amplitudes and realizations. (JPG)

S10 Fig. Snapshots of functional effects under other noise amplitudes for one realization. (A) Noise amplitude = 10^{-8} , Pearson's $r = 0.67$, FDR-corrected $p < 0.01$. (B) Noise amplitude = 10^{-6} , Pearson's $r = 0.79$, FDR-corrected $p < 0.01$. (C) Noise amplitude = 10^{-4} , Pearson's $r = 0.94$, FDR-corrected $p < 0.01$. (D) Noise amplitude = 10^{-2} , Pearson's $r = 0.16$, FDR-corrected $p = 0.15$. The gray lines represent the linear fits of data points estimated by ordinary least squares. These results are in line with the trend shown in Fig 6C. (JPG)

S11 Fig. P-values of Pearson correlation coefficients between structural effects and structural degree as a function of noise amplitude. The blue dots at each noise amplitude represent the 30 realizations of p-values. The red horizontal line indicates the position where the p-value is equal to 0.05. FDR correction was performed for p-values across all noise amplitudes and realizations. (JPG)

S12 Fig. Snapshots of structural effects under other noise amplitudes for one realization. (A) Noise amplitude = 10^{-8} , Pearson's $r = -0.56$, FDR-corrected $p < 0.01$. (B) Noise amplitude = 10^{-6} , Pearson's $r = -0.39$, FDR-corrected $p < 0.01$. (C) Noise amplitude = 10^{-4} , Pearson's $r = 0.08$, FDR-corrected $p = 0.52$. (D) Noise amplitude = 10^{-2} , Pearson's $r = 0.32$, FDR-corrected $p < 0.01$. The gray lines represent the linear fits of data points estimated by ordinary least squares. These results are consistent with the trend shown in Fig 7C. (JPG)

S13 Fig. Locations of cognitive systems in terms of functional and structural effects under other noise amplitudes. (A) Noise amplitude = 10^{-8} . (B) Noise amplitude = 10^{-7} . (C) Noise amplitude = 10^{-5} . (D) Noise amplitude = 10^{-4} . (E) Noise amplitude = 10^{-2} . Note that stimulated brain regions are grouped into 4 cognitive systems with different colors. The colored areas represent the convex hulls of data points in the systems. The points reflect the measures averaged over 30 realizations. (JPG)

Author Contributions

Conceptualization: Yi Zheng, Shaoting Tang.

Funding acquisition: Shaoting Tang.

Investigation: Yi Zheng, Shaoting Tang, Hongwei Zheng, Xin Wang, Longzhao Liu, Yaqian Yang, Yi Zhen, Zhiming Zheng.

Methodology: Yi Zheng, Shaoting Tang, Hongwei Zheng, Xin Wang.

Supervision: Shaoting Tang, Hongwei Zheng.

Visualization: Yi Zheng, Longzhao Liu.

Writing – original draft: Yi Zheng.

Writing – review & editing: Yi Zheng, Shaoting Tang, Hongwei Zheng.

References

1. Bullmore E, Sporns O. Complex brain networks: graph theoretical analysis of structural and functional systems. *Nature reviews neuroscience*. 2009; 10(3):186–198. <https://doi.org/10.1038/nrn2575> PMID: 19190637
2. Bassett DS, Sporns O. Network neuroscience. *Nature neuroscience*. 2017; 20(3):353–364. <https://doi.org/10.1038/nn.4502> PMID: 28230844
3. Vohryzek J, Cabral J, Vuust P, Deco G, Kringelbach ML. Understanding brain states across spacetime informed by whole-brain modelling. *Philosophical Transactions of the Royal Society A*. 2022; 380(2227):20210247. <https://doi.org/10.1098/rsta.2021.0247> PMID: 35599554
4. Fanselow MS, Poulos AM. The neuroscience of mammalian associative learning. *Annual review of psychology*. 2005; 56(1):207–234. <https://doi.org/10.1146/annurev.psych.56.091103.070213> PMID: 15709934
5. Wang XJ. Probabilistic decision making by slow reverberation in cortical circuits. *Neuron*. 2002; 36(5):955–968. [https://doi.org/10.1016/S0896-6273\(02\)01092-9](https://doi.org/10.1016/S0896-6273(02)01092-9) PMID: 12467598
6. Schacter DL, Addis DR, Hassabis D, Martin VC, Spreng RN, Szpunar KK. The future of memory: remembering, imagining, and the brain. *Neuron*. 2012; 76(4):677–694. <https://doi.org/10.1016/j.neuron.2012.11.001> PMID: 23177955
7. Kim J, Roberts J, Robinson P. Dynamics of epileptic seizures: evolution, spreading, and suppression. *Journal of theoretical biology*. 2009; 257(4):527–532. <https://doi.org/10.1016/j.jtbi.2008.12.009> PMID: 19150365
8. Proix T, Jirsa VK, Bartolomei F, Guye M, Truccolo W. Predicting the spatiotemporal diversity of seizure propagation and termination in human focal epilepsy. *Nature communications*. 2018; 9(1):1–15. <https://doi.org/10.1038/s41467-018-02973-y> PMID: 29540685
9. Beynel L, Powers JP, Appelbaum LG. Effects of repetitive transcranial magnetic stimulation on resting-state connectivity: A systematic review. *Neuroimage*. 2020; 211:116596. <https://doi.org/10.1016/j.neuroimage.2020.116596> PMID: 32014552
10. Polanía R, Nitsche MA, Ruff CC. Studying and modifying brain function with non-invasive brain stimulation. *Nature neuroscience*. 2018; 21(2):174–187. <https://doi.org/10.1038/s41593-017-0054-4> PMID: 29311747
11. Krack P, Hariz MI, Baunez C, Guridi J, Obeso JA. Deep brain stimulation: from neurology to psychiatry? *Trends in neurosciences*. 2010; 33(10):474–484. <https://doi.org/10.1016/j.tins.2010.07.002> PMID: 20832128
12. Okun MS. Deep-brain stimulation for Parkinson's disease. *New England Journal of Medicine*. 2012; 367(16):1529–1538. <https://doi.org/10.1056/NEJMct1208070> PMID: 23075179
13. Laxton AW, Lozano AM. Deep brain stimulation for the treatment of Alzheimer disease and dementias. *World neurosurgery*. 2013; 80(3-4):S28–e1. <https://doi.org/10.1016/j.wneu.2012.06.028> PMID: 22722036
14. DeGiorgio CM, Krahl SE. Neurostimulation for drug-resistant epilepsy. *Continuum: Lifelong Learning in Neurology*. 2013; 19(3 Epilepsy):743. <https://doi.org/10.1212/01.CON.0000431397.61970.2b> PMID: 23739108
15. Oberman LM, Rotenberg A, Pascual-Leone A. Use of transcranial magnetic stimulation in autism spectrum disorders. *Journal of autism and developmental disorders*. 2015; 45(2):524–536. <https://doi.org/10.1007/s10803-013-1960-2> PMID: 24127165
16. Osoegawa C, Gomes JS, Grigolon RB, Brietzke E, Gadelha A, Lacerda AL, et al. Non-invasive brain stimulation for negative symptoms in schizophrenia: an updated systematic review and meta-analysis. *Schizophrenia research*. 2018; 197:34–44. <https://doi.org/10.1016/j.schres.2018.01.010> PMID: 29397282
17. Shafi MM, Westover MB, Fox MD, Pascual-Leone A. Exploration and modulation of brain network interactions with noninvasive brain stimulation in combination with neuroimaging. *European Journal of Neuroscience*. 2012; 35(6):805–825. <https://doi.org/10.1111/j.1460-9568.2012.08035.x> PMID: 22429242

18. To WT, De Ridder D, Hart J Jr, Vanneste S. Changing brain networks through non-invasive neuromodulation. *Frontiers in human neuroscience*. 2018; 12:128. <https://doi.org/10.3389/fnhum.2018.00128> PMID: 29706876
19. Baldermann JC, Melzer C, Zapf A, Kohl S, Timmermann L, Tittgemeyer M, et al. Connectivity profile predictive of effective deep brain stimulation in obsessive-compulsive disorder. *Biological psychiatry*. 2019; 85(9):735–743. <https://doi.org/10.1016/j.biopsych.2018.12.019> PMID: 30777287
20. Momi D, Ozdemir RA, Tadayon E, Boucher P, Shafi MM, Pascual-Leone A, et al. Network-level macroscale structural connectivity predicts propagation of transcranial magnetic stimulation. *Neuroimage*. 2021; 229:117698. <https://doi.org/10.1016/j.neuroimage.2020.117698> PMID: 33385561
21. Bergmann TO. Brain state-dependent brain stimulation. *Frontiers in psychology*. 2018; 9:2108. <https://doi.org/10.3389/fpsyg.2018.02108> PMID: 30443236
22. Bradley C, Nydam AS, Dux PE, Mattingley JB. State-dependent effects of neural stimulation on brain function and cognition. *Nature Reviews Neuroscience*. 2022; p. 1–17. PMID: 35577959
23. Massimini M, Ferrarelli F, Huber R, Esser SK, Singh H, Tononi G. Breakdown of cortical effective connectivity during sleep. *Science*. 2005; 309(5744):2228–2232. <https://doi.org/10.1126/science.1117256> PMID: 16195466
24. Feredoes E, Heinen K, Weiskopf N, Ruff C, Driver J. Causal evidence for frontal involvement in memory target maintenance by posterior brain areas during distracter interference of visual working memory. *Proceedings of the National Academy of Sciences*. 2011; 108(42):17510–17515. <https://doi.org/10.1073/pnas.1106439108> PMID: 21987824
25. van Bueren NE, Reed TL, Nguyen V, Sheffield JG, van der Ven SH, Osborne MA, et al. Personalized brain stimulation for effective neurointervention across participants. *PLoS computational biology*. 2021; 17(9):e1008886. <https://doi.org/10.1371/journal.pcbi.1008886> PMID: 34499639
26. López-Alonso V, Cheeran B, Río-Rodríguez D, Fernández-del Olmo M. Inter-individual variability in response to non-invasive brain stimulation paradigms. *Brain stimulation*. 2014; 7(3):372–380. <https://doi.org/10.1016/j.brs.2014.02.004> PMID: 24630849
27. Papadopoulos L, Lynn CW, Battaglia D, Bassett DS. Relations between large-scale brain connectivity and effects of regional stimulation depend on collective dynamical state. *PLoS computational biology*. 2020; 16(9):e1008144. <https://doi.org/10.1371/journal.pcbi.1008144> PMID: 32886673
28. Faisal AA, Selen LP, Wolpert DM. Noise in the nervous system. *Nature reviews neuroscience*. 2008; 9(4):292–303. <https://doi.org/10.1038/nrn2258> PMID: 18319728
29. Deco G, Jirsa V, McIntosh AR, Sporns O, Kötter R. Key role of coupling, delay, and noise in resting brain fluctuations. *Proceedings of the National Academy of Sciences*. 2009; 106(25):10302–10307. <https://doi.org/10.1073/pnas.0901831106> PMID: 19497858
30. Ghosh A, Rho Y, McIntosh AR, Kötter R, Jirsa VK. Noise during rest enables the exploration of the brain's dynamic repertoire. *PLoS computational biology*. 2008; 4(10):e1000196. <https://doi.org/10.1371/journal.pcbi.1000196> PMID: 18846206
31. Brunel N, Hansel D. How noise affects the synchronization properties of recurrent networks of inhibitory neurons. *Neural computation*. 2006; 18(5):1066–1110. <https://doi.org/10.1162/neco.2006.18.5.1066> PMID: 16595058
32. Touboul JD, Piette C, Venance L, Ermentrout GB. Noise-induced synchronization and antiresonance in interacting excitable systems: applications to deep brain stimulation in Parkinson's disease. *Physical Review X*. 2020; 10(1):011073. <https://doi.org/10.1103/PhysRevX.10.011073>
33. Ross B, Miyazaki T, Fujioka T. Interference in dichotic listening: the effect of contralateral noise on oscillatory brain networks. *European Journal of Neuroscience*. 2012; 35(1):106–118. <https://doi.org/10.1111/j.1460-9568.2011.07935.x> PMID: 22171970
34. Gleiss S, Kayser C. Acoustic noise improves visual perception and modulates occipital oscillatory states. *Journal of Cognitive Neuroscience*. 2014; 26(4):699–711. https://doi.org/10.1162/jocn_a_00524 PMID: 24236698
35. Seghier ML, Price CJ. Interpreting and utilising intersubject variability in brain function. *Trends in cognitive sciences*. 2018; 22(6):517–530. <https://doi.org/10.1016/j.tics.2018.03.003> PMID: 29609894
36. Miniussi C, Harris JA, Ruzzoli M. Modelling non-invasive brain stimulation in cognitive neuroscience. *Neuroscience & Biobehavioral Reviews*. 2013; 37(8):1702–1712. <https://doi.org/10.1016/j.neubiorev.2013.06.014> PMID: 23827785
37. Muldoon SF, Pasqualetti F, Gu S, Cieslak M, Grafton ST, Vettel JM, et al. Stimulation-based control of dynamic brain networks. *PLoS computational biology*. 2016; 12(9):e1005076. <https://doi.org/10.1371/journal.pcbi.1005076> PMID: 27611328

38. Spiegler A, Hansen EC, Bernard C, McIntosh AR, Jirsa VK. Selective activation of resting-state networks following focal stimulation in a connectome-based network model of the human brain. *eneuro*. 2016; 3(5). <https://doi.org/10.1523/ENEURO.0068-16.2016> PMID: 27752540
39. Kunze T, Hunold A, Haueisen J, Jirsa V, Spiegler A. Transcranial direct current stimulation changes resting state functional connectivity: A large-scale brain network modeling study. *Neuroimage*. 2016; 140:174–187. <https://doi.org/10.1016/j.neuroimage.2016.02.015> PMID: 26883068
40. Gollo LL, Roberts JA, Cocchi L. Mapping how local perturbations influence systems-level brain dynamics. *Neuroimage*. 2017; 160:97–112. <https://doi.org/10.1016/j.neuroimage.2017.01.057> PMID: 28126550
41. Bansal K, Medaglia JD, Bassett DS, Vettel JM, Muldoon SF. Data-driven brain network models differentiate variability across language tasks. *PLoS computational biology*. 2018; 14(10):e1006487. <https://doi.org/10.1371/journal.pcbi.1006487> PMID: 30332401
42. Betzel RF, Bassett DS. Specificity and robustness of long-distance connections in weighted, interareal connectomes. *Proceedings of the National Academy of Sciences*. 2018; 115(21):E4880–E4889. <https://doi.org/10.1073/pnas.1720186115> PMID: 29739890
43. Betzel RF, Medaglia JD, Bassett DS. Diversity of meso-scale architecture in human and non-human connectomes. *Nature communications*. 2018; 9(1):1–14. <https://doi.org/10.1038/s41467-017-02681-z> PMID: 29367627
44. Cammoun L, Gigandet X, Meskaldji D, Thiran JP, Sporns O, Do KQ, et al. Mapping the human connectome at multiple scales with diffusion spectrum MRI. *Journal of neuroscience methods*. 2012; 203(2):386–397. <https://doi.org/10.1016/j.jneumeth.2011.09.031> PMID: 22001222
45. Betzel RF, Medaglia JD, Papadopoulos L, Baum GL, Gur R, Gur R, et al. The modular organization of human anatomical brain networks: Accounting for the cost of wiring. *Network Neuroscience*. 2017; 1(1):42–68. https://doi.org/10.1162/NETN_a_00002 PMID: 30793069
46. Hlinka J, Coombes S. Using computational models to relate structural and functional brain connectivity. *European Journal of Neuroscience*. 2012; 36(2):2137–2145. <https://doi.org/10.1111/j.1460-9568.2012.08081.x> PMID: 22805059
47. Murray JD, Demirtaş M, Anticevic A. Biophysical modeling of large-scale brain dynamics and applications for computational psychiatry. *Biological Psychiatry: Cognitive Neuroscience and Neuroimaging*. 2018; 3(9):777–787. <https://doi.org/10.1016/j.bpsc.2018.07.004> PMID: 30093344
48. Wilson HR, Cowan JD. Excitatory and inhibitory interactions in localized populations of model neurons. *Biophysical journal*. 1972; 12(1):1–24. [https://doi.org/10.1016/S0006-3495\(72\)86068-5](https://doi.org/10.1016/S0006-3495(72)86068-5) PMID: 4332108
49. Roberts JA, Gollo LL, Abeysuriya RG, Roberts G, Mitchell PB, Woolrich MW, et al. Metastable brain waves. *Nature communications*. 2019; 10(1):1–17. <https://doi.org/10.1038/s41467-019-08999-0> PMID: 30837462
50. Bansal K, Garcia JO, Tompson SH, Verstynen T, Vettel JM, Muldoon SF. Cognitive chimera states in human brain networks. *Science Advances*. 2019; 5(4):eaau8535. <https://doi.org/10.1126/sciadv.aau8535> PMID: 30949576
51. Jenkinson N, Brown P. New insights into the relationship between dopamine, beta oscillations and motor function. *Trends in neurosciences*. 2011; 34(12):611–618. <https://doi.org/10.1016/j.tins.2011.09.003> PMID: 22018805
52. Abbasi O, Gross J. Beta-band oscillations play an essential role in motor–auditory interactions. *Human brain mapping*. 2020; 41(3):656–665. <https://doi.org/10.1002/hbm.24830> PMID: 31639252
53. Dickinson A, DiStefano C, Senturk D, Jeste SS. Peak alpha frequency is a neural marker of cognitive function across the autism spectrum. *European Journal of Neuroscience*. 2018; 47(6):643–651. <https://doi.org/10.1111/ejn.13645> PMID: 28700096
54. Rodriguez-Larios J, Alaerts K. Tracking transient changes in the neural frequency architecture: harmonic relationships between theta and alpha peaks facilitate cognitive performance. *Journal of Neuroscience*. 2019; 39(32):6291–6298. <https://doi.org/10.1523/JNEUROSCI.2919-18.2019> PMID: 31175211
55. Kramer MA, Eden UT, Cash SS, Kolaczyk ED. Network inference with confidence from multivariate time series. *Physical Review E*. 2009; 79(6):061916. <https://doi.org/10.1103/PhysRevE.79.061916> PMID: 19658533
56. Feldt S, Osterhage H, Mormann F, Lehnertz K, Żochowski M. Internetwork and intranetwork communications during bursting dynamics: applications to seizure prediction. *Physical Review E*. 2007; 76(2):021920. <https://doi.org/10.1103/PhysRevE.76.021920> PMID: 17930078
57. Deco G, Jirsa VK, McIntosh AR. Resting brains never rest: computational insights into potential cognitive architectures. *Trends in neurosciences*. 2013; 36(5):268–274. <https://doi.org/10.1016/j.tins.2013.03.001> PMID: 23561718

58. Sanz Perl Y, Escrichs A, Tagliazucchi E, Kringelbach ML, Deco G. Strength-dependent perturbation of whole-brain model working in different regimes reveals the role of fluctuations in brain dynamics. *PLOS Computational Biology*. 2022; 18(11):e1010662. <https://doi.org/10.1371/journal.pcbi.1010662> PMID: 36322525
59. Lynn CW, Bassett DS. The physics of brain network structure, function and control. *Nature Reviews Physics*. 2019; 1(5):318–332. <https://doi.org/10.1038/s42254-019-0040-8>
60. van den Heuvel MP, Sporns O. Network hubs in the human brain. *Trends in cognitive sciences*. 2013; 17(12):683–696. <https://doi.org/10.1016/j.tics.2013.09.012> PMID: 24231140
61. Sporns O, Chialvo DR, Kaiser M, Hilgetag CC. Organization, development and function of complex brain networks. *Trends in cognitive sciences*. 2004; 8(9):418–425. <https://doi.org/10.1016/j.tics.2004.07.008> PMID: 15350243
62. Power JD, Cohen AL, Nelson SM, Wig GS, Barnes KA, Church JA, et al. Functional network organization of the human brain. *Neuron*. 2011; 72(4):665–678. <https://doi.org/10.1016/j.neuron.2011.09.006> PMID: 22099467
63. Henrie JA, Shapley R. LFP power spectra in V1 cortex: the graded effect of stimulus contrast. *Journal of neurophysiology*. 2005; 94(1):479–490. <https://doi.org/10.1152/jn.00919.2004> PMID: 15703230
64. McDonnell MD, Ward LM. The benefits of noise in neural systems: bridging theory and experiment. *Nature Reviews Neuroscience*. 2011; 12(7):415–425. <https://doi.org/10.1038/nrn3061> PMID: 21685932
65. Traub RD, Wong RK. Cellular mechanism of neuronal synchronization in epilepsy. *Science*. 1982; 216(4547):745–747. <https://doi.org/10.1126/science.7079735> PMID: 7079735
66. Slooter A, Vriens E, Leijten F, Spijkstra J, Girbes A, van Huffelen A, et al. Seizure detection in adult ICU patients based on changes in EEG synchronization likelihood. *Neurocritical care*. 2006; 5(3):186–192. <https://doi.org/10.1385/NCC:5:3:186> PMID: 17290086
67. Dinstein I, Heeger DJ, Lorenzi L, Minschew NJ, Malach R, Behrmann M. Unreliable evoked responses in autism. *Neuron*. 2012; 75(6):981–991. <https://doi.org/10.1016/j.neuron.2012.07.026> PMID: 22998867
68. Weinger PM, Zemon V, Soorya L, Gordon J. Low-contrast response deficits and increased neural noise in children with autism spectrum disorder. *Neuropsychologia*. 2014; 63:10–18. <https://doi.org/10.1016/j.neuropsychologia.2014.07.031> PMID: 25107679
69. Winterer G, Weinberger DR. Genes, dopamine and cortical signal-to-noise ratio in schizophrenia. *Trends in neurosciences*. 2004; 27(11):683–690. <https://doi.org/10.1016/j.tins.2004.08.002> PMID: 15474169
70. Tran TT, Rolle CE, Gazzaley A, Voytek B. Linked sources of neural noise contribute to age-related cognitive decline. *Journal of cognitive neuroscience*. 2020; 32(9):1813–1822. https://doi.org/10.1162/jocn_a_01584 PMID: 32427069
71. González-Villar AJ, Samartin-Veiga N, Arias M, Carrillo-de-la Peña MT. Increased neural noise and impaired brain synchronization in fibromyalgia patients during cognitive interference. *Scientific reports*. 2017; 7(1):1–8. <https://doi.org/10.1038/s41598-017-06103-4> PMID: 28724985
72. Voytek B, Knight RT. Dynamic network communication as a unifying neural basis for cognition, development, aging, and disease. *Biological psychiatry*. 2015; 77(12):1089–1097. <https://doi.org/10.1016/j.biopsych.2015.04.016> PMID: 26005114
73. Kitajo K, Nozaki D, Ward LM, Yamamoto Y. Behavioral stochastic resonance within the human brain. *Physical Review Letters*. 2003; 90(21):218103. <https://doi.org/10.1103/PhysRevLett.90.218103> PMID: 12786595
74. Moss F, Ward LM, Sannita WG. Stochastic resonance and sensory information processing: a tutorial and review of application. *Clinical neurophysiology*. 2004; 115(2):267–281. <https://doi.org/10.1016/j.clinph.2003.09.014> PMID: 14744566
75. Hearne LJ, Lin HY, Sanz-Leon P, Tseng WYI, Gau SSF, Roberts JA, et al. ADHD symptoms map onto noise-driven structure–function decoupling between hub and peripheral brain regions. *Molecular Psychiatry*. 2021; 26(8):4036–4045. <https://doi.org/10.1038/s41380-019-0554-6> PMID: 31666679
76. Hermundstad AM, Brown KS, Bassett DS, Aminoff EM, Frithsen A, Johnson A, et al. Structurally-constrained relationships between cognitive states in the human brain. *PLoS computational biology*. 2014; 10(5):e1003591. <https://doi.org/10.1371/journal.pcbi.1003591> PMID: 24830758
77. Wang J, Noh GJ, Choi BM, Ku SW, Joo P, Jung WS, et al. Suppressed neural complexity during ketamine- and propofol-induced unconsciousness. *Neuroscience letters*. 2017; 653:320–325. <https://doi.org/10.1016/j.neulet.2017.05.045> PMID: 28572032
78. Varley TF, Denny V, Sporns O, Patania A. Topological analysis of differential effects of ketamine and propofol anaesthesia on brain dynamics. *Royal Society open science*. 2021; 8(6):201971. <https://doi.org/10.1098/rsos.201971> PMID: 34168888

79. Sellers KK, Bennett DV, Hutt A, Fröhlich F. Anesthesia differentially modulates spontaneous network dynamics by cortical area and layer. *Journal of neurophysiology*. 2013; 110(12):2739–2751. <https://doi.org/10.1152/jn.00404.2013> PMID: 24047911
80. Sellers KK, Bennett DV, Hutt A, Williams JH, Fröhlich F. Awake vs. anesthetized: layer-specific sensory processing in visual cortex and functional connectivity between cortical areas. *Journal of neurophysiology*. 2015; 113(10):3798–3815. <https://doi.org/10.1152/jn.00923.2014> PMID: 25833839
81. Murriss SR, Arsenault JT, Vanduffel W. Frequency- and state-dependent network effects of electrical stimulation targeting the ventral tegmental area in macaques. *Cerebral Cortex*. 2020; 30(8):4281–4296. <https://doi.org/10.1093/cercor/bhaa007> PMID: 32279076
82. Premereur E, Van Dromme IC, Romero MC, Vanduffel W, Janssen P. Effective connectivity of depth-structure-selective patches in the lateral bank of the macaque intraparietal sulcus. *PLoS biology*. 2015; 13(2):e1002072. <https://doi.org/10.1371/journal.pbio.1002072> PMID: 25689048
83. Suárez LE, Markello RD, Betzel RF, Misic B. Linking structure and function in macroscale brain networks. *Trends in Cognitive Sciences*. 2020; 24(4):302–315. <https://doi.org/10.1016/j.tics.2020.01.008> PMID: 32160567
84. Yang Y, Zheng Z, Liu L, Zheng H, Zhen Y, Zheng Y, et al. Enhanced brain structure-function tethering in transmodal cortex revealed by high-frequency eigenmodes. *bioRxiv*. 2022; p. 2022–07.
85. Honey CJ, Sporns O, Cammoun L, Gigandet X, Thiran JP, Meuli R, et al. Predicting human resting-state functional connectivity from structural connectivity. *Proceedings of the National Academy of Sciences*. 2009; 106(6):2035–2040. <https://doi.org/10.1073/pnas.0811168106> PMID: 19188601
86. Abdelnour F, Voss HU, Raj A. Network diffusion accurately models the relationship between structural and functional brain connectivity networks. *Neuroimage*. 2014; 90:335–347. <https://doi.org/10.1016/j.neuroimage.2013.12.039> PMID: 24384152
87. Seguin C, Van Den Heuvel MP, Zalesky A. Navigation of brain networks. *Proceedings of the National Academy of Sciences*. 2018; 115(24):6297–6302. <https://doi.org/10.1073/pnas.1801351115> PMID: 29848631
88. Yang Y, Qiao S, Sani OG, Sedillo JI, Ferrentino B, Pesaran B, et al. Modelling and prediction of the dynamic responses of large-scale brain networks during direct electrical stimulation. *Nature biomedical engineering*. 2021; 5(4):324–345. <https://doi.org/10.1038/s41551-020-00666-w> PMID: 33526909
89. Boccaletti S, Latora V, Moreno Y, Chavez M, Hwang DU. Complex networks: Structure and dynamics. *Physics reports*. 2006; 424(4-5):175–308. <https://doi.org/10.1016/j.physrep.2005.10.009>
90. Gu S, Pasqualetti F, Cieslak M, Telesford QK, Yu AB, Kahn AE, et al. Controllability of structural brain networks. *Nature communications*. 2015; 6(1):1–10. <https://doi.org/10.1038/ncomms9414> PMID: 26423222
91. Khambhati AN, Kahn AE, Costantini J, Ezzyat Y, Solomon EA, Gross RE, et al. Functional control of electrophysiological network architecture using direct neurostimulation in humans. *Network Neuroscience*. 2019; 3(3):848–877. https://doi.org/10.1162/netn_a_00089 PMID: 31410383
92. Gramann K, Jung TP, Ferris DP, Lin CT, Makeig S. Toward a new cognitive neuroscience: modeling natural brain dynamics; 2014.
93. Criscuolo A, Schwartz M, Kotz SA. Cognition through the lens of a body–brain dynamic system. *Trends in neurosciences*. 2022;.
94. Bi Xa, Zhao J, Xu Q, Sun Q, Wang Z. Abnormal functional connectivity of resting state network detection based on linear ICA analysis in autism spectrum disorder. *Frontiers in physiology*. 2018; 9:475. <https://doi.org/10.3389/fphys.2018.00475> PMID: 29867534
95. Li S, Hu N, Zhang W, Tao B, Dai J, Gong Y, et al. Dysconnectivity of multiple brain networks in schizophrenia: a meta-analysis of resting-state functional connectivity. *Frontiers in psychiatry*. 2019; 10:482. <https://doi.org/10.3389/fpsy.2019.00482> PMID: 31354545
96. Long Y, Liu Z, Chan CKY, Wu G, Xue Z, Pan Y, et al. Altered temporal variability of local and large-scale resting-state brain functional connectivity patterns in schizophrenia and bipolar disorder. *Frontiers in psychiatry*. 2020; 11:422. <https://doi.org/10.3389/fpsy.2020.00422> PMID: 32477194
97. Deco G, Tononi G, Boly M, Kringelbach ML. Rethinking segregation and integration: contributions of whole-brain modelling. *Nature Reviews Neuroscience*. 2015; 16(7):430–439. <https://doi.org/10.1038/nrn3963> PMID: 26081790
98. Cohen JR, D'Esposito M. The segregation and integration of distinct brain networks and their relationship to cognition. *Journal of Neuroscience*. 2016; 36(48):12083–12094. <https://doi.org/10.1523/JNEUROSCI.2965-15.2016> PMID: 27903719
99. Cabral J, Kringelbach ML, Deco G. Functional connectivity dynamically evolves on multiple time-scales over a static structural connectome: Models and mechanisms. *NeuroImage*. 2017; 160:84–96. <https://doi.org/10.1016/j.neuroimage.2017.03.045> PMID: 28343985

100. Reato D, Rahman A, Bikson M, Parra LC. Effects of weak transcranial alternating current stimulation on brain activity—a review of known mechanisms from animal studies. *Frontiers in human neuroscience*. 2013; 7:687. <https://doi.org/10.3389/fnhum.2013.00687> PMID: 24167483
101. Wang P, Kong R, Kong X, Liégeois R, Orban C, Deco G, et al. Inversion of a large-scale circuit model reveals a cortical hierarchy in the dynamic resting human brain. *Science advances*. 2019; 5(1): eaat7854. <https://doi.org/10.1126/sciadv.aat7854> PMID: 30662942
102. Wang XJ. Macroscopic gradients of synaptic excitation and inhibition in the neocortex. *Nature Reviews Neuroscience*. 2020; 21(3):169–178. <https://doi.org/10.1038/s41583-020-0262-x> PMID: 32029928
103. Kong X, Kong R, Orban C, Wang P, Zhang S, Anderson K, et al. Sensory-motor cortices shape functional connectivity dynamics in the human brain. *Nature communications*. 2021; 12(1):1–15. <https://doi.org/10.1038/s41467-021-26704-y> PMID: 34737302
104. Shine JM, Müller EJ, Munn B, Cabral J, Moran RJ, Breakspear M. Computational models link cellular mechanisms of neuromodulation to large-scale neural dynamics. *Nature neuroscience*. 2021; 24(6):765–776. <https://doi.org/10.1038/s41593-021-00824-6> PMID: 33958801
105. Tripp EA, Fu F, Pauls SD. Evolutionary Kuramoto dynamics. *Proceedings of the Royal Society B*. 2022; 289(1986):20220999. <https://doi.org/10.1098/rspb.2022.0999> PMID: 36350204
106. Carhart-Harris RL, Leech R, Hellyer PJ, Shanahan M, Feilding A, Tagliazucchi E, et al. The entropic brain: a theory of conscious states informed by neuroimaging research with psychedelic drugs. *Frontiers in human neuroscience*. 2014; p. 20. <https://doi.org/10.3389/fnhum.2014.00020> PMID: 24550805